Comparison of Miocene to early Pleistocene-aged *Castor californicus* (Rodentia: Castoridae) to extant beavers and implications for the evolution of *Castor* in North America

Kelly E. Lubbers and Joshua X. Samuels

ABSTRACT

The beaver, genus *Castor*, is represented in North America today by *Castor canadensis* and in Eurasia by *C. fiber*. Historically, the fossil Miocene to early Pleistocene-aged North American beaver *C. californicus* has been considered a distinct species from *C. canadensis* due to its larger size. In this study, we test the hypothesis that the morphology of Miocene to early Pleistocene-aged fossils of *C. californicus* differs from that of the extant *C. canadensis*. Specimens of fossil and extant *Castor* were compared using 2D geometric morphometrics of skull and dentary material and linear measurements of postcranial material to analyze morphological differences between species and determine whether *C. californicus* fits within the range of intraspecific variation seen in *C. canadensis*. Results show that *C. canadensis* is highly variable in both skull and postcranial morphology, and *C. californicus* falls largely within the range of variation seen within the extant species. The morphological similarities between the two species suggest that they can be treated as ecological analogs and may represent change in a single species through time, although a rigorous evaluation of whether they are conspecific will require more data.

Kelly E. Lubbers. The Mammoth Site, Hot Springs, South Dakota 57747, USA and Department of Geosciences, East Tennessee State University, Johnson City, Tennessee 37614, USA. kellyl@mammothsite.org

Joshua X. Samuels. Department of Geosciences, East Tennessee State University, Johnson City, Tennessee 37614, USA and Don Sundquist Center of Excellence in Paleontology, East Tennessee State University, Johnson City, Tennessee, 37614, USA. samuelsjx@etsu.edu

INTRODUCTION

Beavers (family Castoridae) first appeared in North America during the late Eocene and from there dispersed into Eurasia (Korth, 1994; Flynn and Jacobs, 2008). The fossil record of beavers includes approximately 30 genera, with diverse lineages adapted to fossorial, terrestrial, and semi-aquatic lifestyles (Martin and Bennett, 1977; Martin, 1989; Korth, 1994; Rybczynski, 2007; Samuels and Van Valkenburgh, 2008; Samuels and Van Valkenburgh, 2009; Calede, 2022). The semi-aquatic lineage of beavers likely arose in the late Oligocene (Korth and Samuels, 2015; Calede, 2022), and members of both Castorinae and Castoroidinae diversified greatly in the Miocene (Rybczynski, 2007; Rybczynski et al., 2010). The genus *Castor* likely appeared in the late Miocene, as represented by *Castor neglectus* from Germany (Hugueney, 1999; Flynn and Jacobs, 2008). Little is known about the dispersals of *Castor* between North America and Eurasia, though it is likely those migrations were facilitated by the Bering land bridge throughout the Cenozoic (Rybczynski, 2007; Flynn and Jacobs, 2008; Samuels and Zancanella, 2011).

Castor has been present in North America since the late Miocene, with the earliest records of *Castor californicus* dating to around 7 m.y.a. (Samuels and Zancanella, 2011). *Castor californicus*

was first discovered in the Kettleman Hills in California (Kellogg, 1911). Kellogg (1911) designated it as a separate species from *C. canadensis* based on features of the upper third molar. Other specimens of *C. californicus*, including skull, postcranial, and dental material, have been discovered and described in Miocene, Pliocene, and early Pleistocene-aged localities across the United States (Figure 1) (Zakrzewski, 1969; Shotwell, 1970; Kurtén and Anderson, 1980; Samuels and Zancanella, 2011). A second species of fossil beaver in North America, *Castor accessor*, was initially described by Hay (1927) and designated as a separate species based on differences in tooth striae lengths compared to *C. californicus* and *C. canadensis* (Hay, 1927; Kurtén and Anderson, 1980). However, due to similarities in size and temporal distribution, *C. accessor* is generally considered a junior synonym of *C. californicus* (Stirton, 1935; Flynn and Jacobs, 2008).

Castor canadensis is one of two extant members of the genus *Castor*, the other being *C. fiber*. Although the two species are similar in morphology, they are genetically and chromosomally different (*C. canadensis* 2n=40, *C. fiber* 2n=48) (Jenkins and Buscher, 1979; Rosell et al., 2005; Brazier et al., 2020). *Castor canadensis* has a distribution extending throughout North America, whereas the distribution of *C. fiber* extends through Eurasia (Jenkins and Buscher, 1979; Halley et al., 2020).
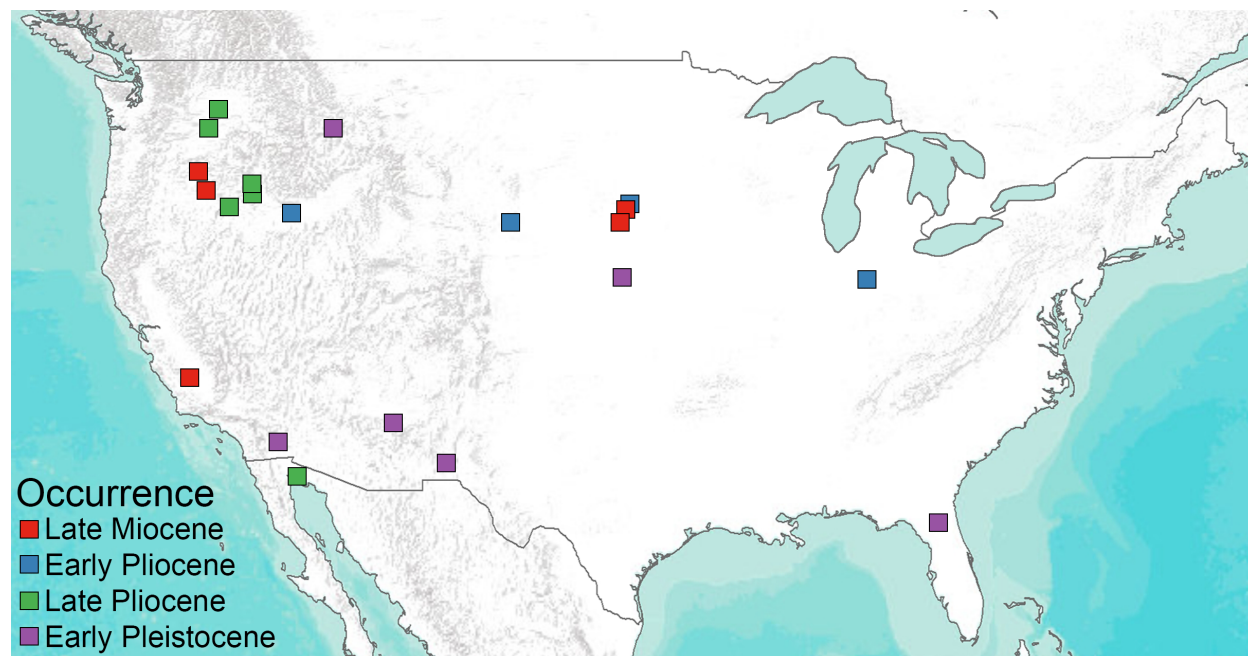

FIGURE 1. Late Miocene through Late Pleistocene fossil localities of *Castor* across North America. Locality points obtained from NOW database of Fossil Mammals.

Since Stirton (1935), *Castor* specimens from the Miocene to early Pleistocene of North America have been referred to as *Castor californicus* (due to shift of the Plio-Pleistocene boundary from 1.8 Ma to 2.5 Ma (Gibbard and Head, 2010), many *C. californicus* specimens originally considered Pliocene are now considered early Pleistocene), whereas those from the late Pleistocene to recent are referred to the living species *C. canadensis* (Kurtén and Anderson, 1980; Flynn and Jacobs, 2008). Although no rigorous analysis has yet been undertaken of this pattern, multiple studies have noted a decrease in size within *Castor* from the Miocene through the Pleistocene of North America (Stirton, 1935; Shotwell, 1970), but otherwise there has been little other morphological change in the taxon (Martin, 1989; Samuels and Zancanella, 2011). This raises the question of whether *C. canadensis* and *C. californicus* are distinct species or represent anagenetic change in a single species over time. The primary purpose of this study is to evaluate whether the Miocene to early Pleistocene-aged *C. californicus* and the late Pleistocene-aged and extant *C. canadensis* are distinct in skull and postcranial morphology. This will improve understanding of the evolution of *Castor* in North America over time and help resolve whether the two species can be treated as conspecific and/or ecological analogs. Based on the age of studied specimens (Pliocene and early Pleistocene), we expect *C. californicus* to either show 1) intermediate morphological features between *C. fiber* and *C. canadensis,* possibly reflecting retention of ancestral *Castor* morphology or evolutionary divergence of Eurasian beavers and North American beavers that increases over time, 2) distinct morphological features that differentiate *C. californicus* from both *C. canadensis* and *C. fiber*, reflecting its status as a distinct species, or 3) strong morphological similarity to *C. canadensis*, reflecting their shared lineage and potential status as chronomorphs of a single synonymous species.

MATERIALS AND METHODS

Cranial Analyses

A total of 67 specimens were used in the analysis of cranial material (Appendix 1). Fifty-nine specimens of *Castor canadensis*, and four of *C. fiber* accounted for the modern sample. For the fossil specimens, three Pliocene and early Pleistocene-aged specimens of *C. californicus* (HAFO 2243, UF 225200, USNM 26154), and one Pleistocene *C. fiber* (FMNH 1537) were used. *Castor fiber*

had limited modern sampling in this analysis due to lack of available specimens in collections visited. While specimens of fossil *C. californicus* are common in North America, limited material was used in this analysis due to fragmentary nature of available fossil specimens.

Forty dentaries of both fossil and modern species were also used for this study (Appendix 2). Modern specimens included 35 *Castor canadensis,* which came from all over North America, and two *C. fiber.* Fossil specimens included two specimens of *C. californicus* (UF 225200, USNM 26154) and one *C. accessor* (UOMNCH 16338), which has been considered synonymous with *C. californicus*, with specimens ranging from Pliocene to early Pleistocene in age.

To minimize the effects of allometry, only adult specimens (approximately 5 years old or greater) were used in the analysis. Adults were selected based on the fusion of the suture between the basioccipital and basisphenoid following Roberson and Shadle (1954). Most dentaries included in the analysis were associated with craniums, however, four isolated dentaries were included from previous identification of specimens being classified as adult. Fossil specimens were selected based on assumptions of age groupings sharing similar characteristics to those of extant beavers; however, an extensive evaluation of age classifications in fossil *Castor californicus* compared to extant *C. canadensis* are outside the scope of this study.

Cranial material was photographed in dorsal, lateral, and ventral views, whereas dentaries were photographed in both lateral and medial views. In dorsal and ventral view specimens were photographed with the palate parallel to the photographic plane, and in lateral view the midline of the palate was aligned perpendicular to the photographic plane. The dentary was photographed with the occlusal surface of the cheek teeth aligned perpendicular to the photographic plane. Scale bars were used with all photos to calibrate known scale when setting landmarks. Specimens were photographed using either a Nikon D810 DSLR camera with an AF-S Micro Nikkor 60 mm lens at a resolution of 7360 x 4912 pixels or a Mercury CyberPix E5205 digital camera at a resolution of 2560 x 1920 pixels. Photographs were taken at a distance using a camera stand to minimize the effects of parallax. Regardless of the camera used, imaged specimens were over 1000 pixels wide, and the linearity of photographs was tested at all magnification levels used. Thin-plate spline (TPS) files were created from JPEG files for all image views using
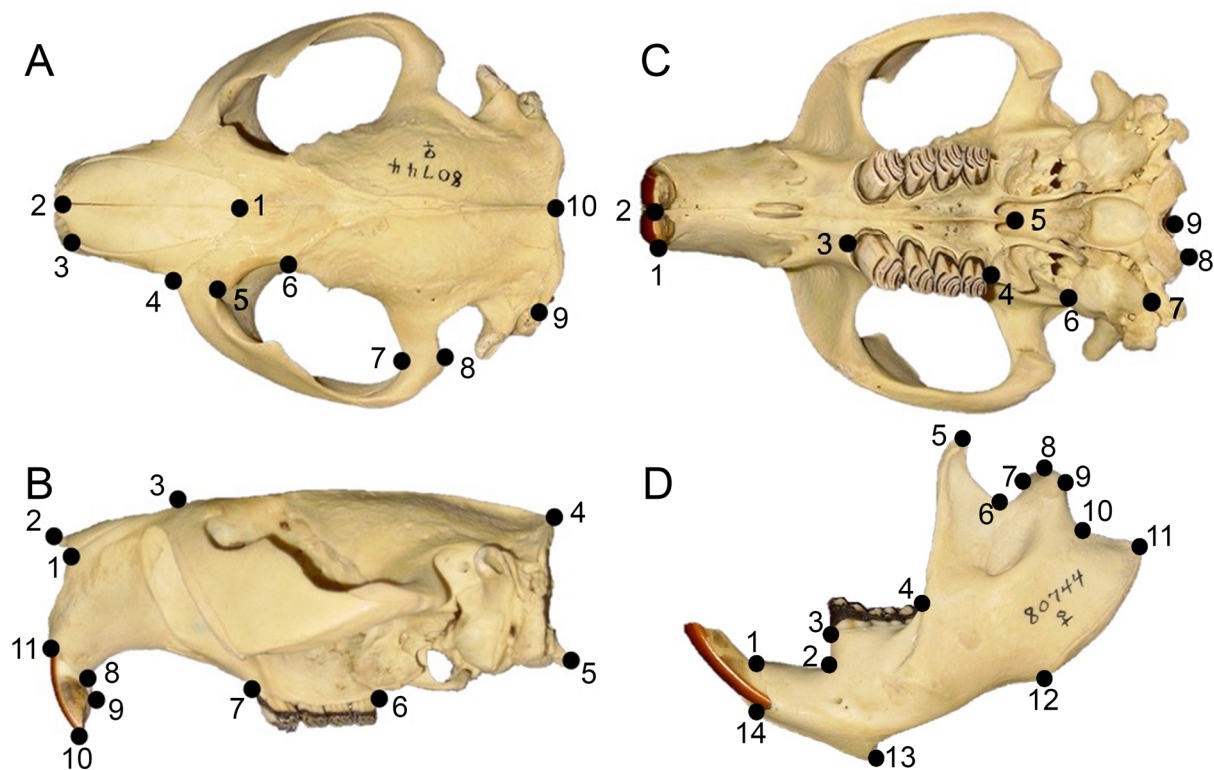
FIGURE 2. Landmark placement for craniums in dorsal (A), lateral (B), and ventral (C) views and dentaries (D) in lateral view on *Castor canadensis* MVZ 80744. Definitions of landmarks are outlined in Table 1 for the cranium and Table 2 for the dentary.

the program tpsUtil32 (v.1.61), in preparation for landmark digitization (Rohlf, 2015). The program tpsDig2 (v. 2.31) was used for digital placement of landmarks on specimen images (Rohlf, 2021). Landmark placement for cranial material (Figure 2; Table 1) followed those previously used in Samuels and Van Valkenburgh (2009) and Rybczynski et al. (2010), and dentary landmarks (Figure 2; Table 2) followed those previously used in Monteiro et al. (2005). To minimize the potential effects of asymmetry, only one side was used for the dorsal and ventral cranial views.

Data Analysis

Landmark data were first analyzed via Relative Warp Analysis (RWA) performed in the tpsRelW program (v 1.70) (Rohlf, 2015). The RWA used generalized least square Procrustes analysis to scale, rotate, and align coordinate sets for each view of the skull and dentary. Two stepwise canonical variates analyses (CVA) were run using partial warp scores and uniform components from all RWA, the first CVA used both *Castor canadensis*

and *C. fiber* as a priori categories with *C. californicus* treated as unknown for the classification phase of the analysis, and the second CVA categorized all three species individually into a priori categories. The classification stage of the CVA was used to determine the accuracy for individual specimens to be assigned into species by the models. Classification occurred in two steps: group classifications and cross-validation, where specimens were excluded from the model and reevaluated using the remaining specimens in the analysis. CVA were run in IBM SPSS Statistics 26.0 and shapes associated with CV scores visualized with tpsRegr (Rohlf, 2011).

The hierarchical cluster analysis was run to examine the phenetic similarity between specimens based on their morphology, without the need for a priori grouping of species. The cluster analysis was run in IBM SPSS Statistics 26.0 using an unweighted paired group means analysis method (UPGMA) and average algorithm with partial warp scores and uniform component scores as variables.

TABLE 1. Landmarks used for geometric morphometric analyses of the skull, following Samuels and Van Valkenburgh, 2009 and Rybczynski et al., 2010.

Landmark #	Placement Description
	Skull Dorsal View
1	Meeting point between nasal and frontal along midsagittal plane
2	Anterior tip of nasal along mid sagittal plane
3	Anterior tip of suture between nasal and premaxilla
4	Anterior tip of suture between premaxilla and maxilla
5	Posterior tip of suture between frontal and jugal
6	Postorbital constriction
7	Most posterior point of temporal fossa along squamosal process of the zygomatic arch
8	Most posterior meeting point between jugal and squamosal process of zygomatic arch
9	Y shaped suture at meeting point of squamosal, parietal, and occipital
10	Most posterior meeting point of sagittal and nuchal crests
	Skull Lateral View
1	Anterior tip of suture between nasal and premaxilla
2	Anterior tip of nasal
3	Meeting point of nasal and frontal along the midsagittal plane
4	Most posterior meeting point of sagittal and nuchal crests
5	Most posterior point of occipital condyle
6	Posterior end of cheek tooth row at the end of the alveolus
7	Anterior end of cheek tooth row at the end of the alveolus
8	Most posterior point of incisor alveolus
9	Posterior edge of upper incisor blade
10	Anterior edge of upper incisor blade
11	Most anterior point of upper incisor alveolus
	Skull Ventral View
1	Lateral edge of upper incisor blade
2	Medial edge of upper incisor blade
3	Anterior end of cheek tooth row
4	Posterior end of cheek tooth row
5	Posterior tip of palate along midsagittal plane
6	Most lateral point of suture between tympanic and squamosal
7	Suture where tympanic and occipital meet
8	Most posterior point of occipital condyle
9	Midsagittal border of foramen magnum

Postcranial Analyses

The analysis of postcranial material used a total of 59 individuals (Appendix 3). Modern specimens included 30 *Castor canadensis* and two *C. fiber*. Fossils included 26 Pliocene-aged specimens identified as *C. californicus* and one Pleistocene-aged *Castor* sp. 64 postcranial characteristics were recorded where possible, measured features (following Samuels and Van Valkenburgh, 2008) included total lengths of bones, midshaft diameters, prominent articular dimensions, and muscle attachments (Table 3). Measurements were collected in millimeters (to 0.01 mm) using Mitutoyo digital calipers.

Measurement data were input to IBM SPSS Statistics 26.0 where descriptive statistics were run for each species. The analysis computed mean, standard deviation, and minimum and maximum values for the measurements of each species. From those data, coefficients of variation were also calculated for each measurement across species. Coefficients of variation compare the range of vari-

TABLE 2. Landmarks used for geometric morphometric analysis of the dentary, following Monteiro et al., 2005.

	Dentary Landmarks
1	Antero-dorsal boarder of incisive alveolus
2	Extreme of diastema invagination
3	Anterior edge of molar tooth row
4	Posterior intersection of molar tooth row with coronoid process
5	Tip of coronoid process
6	Maximum curvature between the coronoid and condylar processes
7	Anterior edge of articular surface of condyle
8	Tip of condylar process
9	Posterior most edge of articular surface of condyle
10	Maximum curvature on the curve between the condylar and angular processes
11	Tip of the angular process
12	Anterior margin of the angular process
13	Posterior extremity of the mandibular symphysis
14	Antero-ventral border of the incisive alveolus

ation seen within groups (Sokal and Braumann, 1980; Cope and Lacy, 1995; Emery-Wetherell and Davis, 2018), in this case species were compared for various postcranial measurements to determine if the level of variation in *Castor calfornicus* fits within the level of intraspecific variation for *C. canadensis*. Only species measurements with more than three specimens were used to calculate coefficients of variation, as fewer than three would represent insufficient sampling. Coefficients of variation were corrected for small sample size bias using the equation previously used in Sokal and Braumann (1980). In addition to the descriptive statistics, an analysis of variance (ANOVA) was run for each of the measurements allowing assessment of differences in mean values between species groups.

Institutional Abbreviations

ETMNHV, East Tennessee State University Museum of Natural History, Zoology Collection (Johnson City, TN, USA); FMNH, Field Museum of Natural History (Chicago, IL, USA); HAFO, Hagerman Fossil Beds National Monument (Hagerman, Idaho, USA); IMNH, Idaho Museum of Natural History (Pocatello, Idaho, USA); LACM, Natural History Museum of Los Angeles County (Los Angeles, California, USA); MVZ, University of California Berkley Museum of Vertebrate Zoology (Berkley, California, USA); UCLA, University of California Los Angeles, Donald R. Dickey Collection (Los Angeles, California, USA); UF, Florida Museum of Natural History (Gainesville, Florida, USA); UOM-NCH, University of Oregon Museum of Natural and Cultural History (Eugene, Oregon, USA); USNM, Smithsonian Institution National Museum of Natural History (Washington D.C., USA); UWBM, University of Washington Burke Museum (Seattle, Washington, USA).

RESULTS

Cranial Analyses

Relative warp analysis. Relative warp analyses were run for each view of the cranium and dentary. The relative warp scores for the dorsal view produced seven significant warps (Eigenvalue >1), explaining 81.5% of the observed shape variation. Dorsal relative warps 1 and 2 showed separation of *Castor fiber* from overlapping *C. canadensis* and *C. californicus* (Figure 3). Dorsal relative warp 1 (DRW1) explained 27.64% of the variation, with *C. fiber* clustered with negative scores whereas *C. californicus* clustered with positive scores. *Castor canadensis* clustered near zero, spanning both positive and negative values. Positive DRW1 scores are associated with shorter nasals, wider occiput, and posteriorly positioned orbit. Negative DRW1 scores are associated with elongated nasals, narrow occiput, and anteriorly positioned orbit. DRW2 explained 17.03% of the variation. Both *C. fiber* and *C. californicus* had positive scores (except for one *C. fiber*), whereas *C. canadensis* displayed a wide range of both positive and negative scores. Positive DRW2 scores are associated with shorter rostrum, narrow posterior cranium, and wider zygomatic arches. Negative DRW2 scores are associated with elongated rostrum, wider occiput, and narrow zygomatic arches.

Relative warp scores for the lateral view produced eight significant warps, explaining 92.73% of the observed shape variation. Relative warps 1 and 3 showed (good?) separation of *Castor fiber* and *C. canadensis* (Figure 4). Lateral relative warp 1 (LRW1) explained 45.97% of the variation, with *C. fiber* having negative scores, *C. californicus* near zero, and *C. canadensis* displaying both positive and negative scores. Negative LRW1 scores are associated with elongated nasals and dorsoventrally shorter occiput. Positive LRW1 scores are associated with shorter nasals and dorsoventrally deeper occiput. LRW3 explained 16.57% of the variation, with *C. fiber* having exclusively negative scores whereas *C. canadensis* and *C. californicus* showed widespread distribution across positive

TABLE 3. Measurements of postcranial elements, following Samuels and Van Valkenburgh, 2008.

Measurement	Definition	Measurement	Definition
ScaL	Length of scapula	TL	Length of tibia
ScaW	Width of scapula	TAPD	Anteroposterior diameter of tibia
ScaAL	Length of acromion process of the scapula	TMLD	Mediolateral diameter of tibia
HL	Length of humerus	TPEAPD	Anteroposterior diameter of tibia proximal epiphysis
HAPD	Anteroposterior diameter of humerus	TPEMLD	Mediolateral diameter of tibia proximal epiphysis
HMLD	Mediolateral diameter of humerus	TDEAPD	Anteroposterior diameter of tibia distal epiphysis
HHD	Diameter of humeral head	TDEMLD	Mediolateral diameter of tibia distal epiphysis
HDAW	Articular width of humeral distal end		
RL	Length of radius	TLOF	Tibia length of fusion to fibula
RAPD	Anteroposterior diameter of radius	FibL	Length of fibula
RMLD	Mediolateral diameter of radius	FibAPD	Anteroposterior diameter of fibula
UL	Length of ulna	FibMLD	Mediolateral diameter of fibula
UAPD	Anteroposterior diameter of ulna	CalcL	Length of calcaneus
UMLD	Mediolateral diameter of ulna	CalcTL	Length of calcaneus tuberosity
ULOL	Length of olecranon process of the ulna	MT1L	Length of 1st metatarsal
MC1L	Length of 1st metacarpal	MT1APD	Anteroposterior diameter of 1st Metatarsal
MC2L	Length of 2nd metacarpal	MT1MLD	Mediolateral diameter of 1st metatarsal
MC3L	Length of 3rd metacarpal	MT2L	Length of 2nd metatarsal
MC3APD	Anteroposterior diameter of 3rd metacarpal	MT2APD	Anteroposterior diameter of 2nd metatarsal
MC3MLD	Mediolateral diameter of 3rd metacarpal	MT2MLD	Mediolateral diameter of 2nd metatarsal
MC4L	Length of 4th metacarpal	MT3L	Length of 3rd metatarsal
MC5L	Length of 5th metacarpal	MT3APD	Anteroposterior diameter of 3rd metatarsal
Mph3p	Length of 3rd manus proximal phalanx	MT3MLD	Mediolateral diameter 3rd metatarsal
Mph3m	Length of 3rd manus medial phalanx	MT4L	Length of 4th metatarsal
Mph3t	Length of 3rd manus terminal phalanx	MT4APD	Anteroposterior diameter of 4th metatarsal
InnomL	Length of innominate (ilium to ischium)	MT4MLD	Mediolateral diameter of 4th metatarsal
IliL	Length of ilium	MT5L	Length of 5th metatarsal
FeL	Length of femur	MT5APD	Anteroposterior diameter of 5th metatarsal
FeAPD	Anteroposterior diameter of femur	MT5MLD	Mediolateral diameter of 5th metatarsal
FeMLD	Mediolateral diameter of femur	Pph3p	Length of 3rd pes proximal phalanx
FeGT	Height of greater trochanter of the femur	Pph3m	Length of 3rd pes medial phalanx
FeHD	Diameter of femoral head	Pph3t	Length of 3rd pes terminal phalanx
FeEB	Femoral epicondylar breadth		

and negative scores. Negative LRW3 scores are associated with the anteroventral extension of the nasals and dorsoventrally shallower occiput. Positive LRW3 scores are associated with shorter nasals and dorsoventrally deeper occiput.

The relative warp scores for the ventral view produced six significant warps, explaining 83.52%

of the observed shape variation (Table 4). None of the six relative warps showed clear separation of species in morphospace and are therefore not described further here.

The relative warp scores for the dentary produced eleven significant warps, explaining 92.87% of the observed shape variation. Relative warps 1
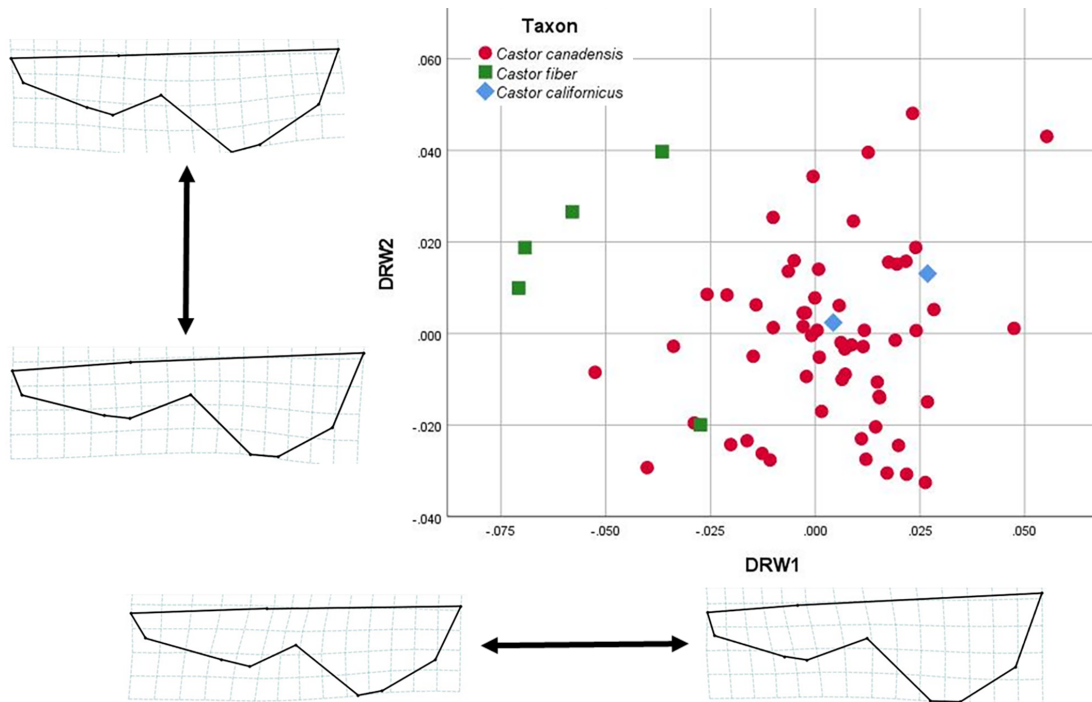
FIGURE 3. Relative warp plot for the dorsal view of the cranium. Axes depict shape variation, associated with landmark deformations, indicated by thin plate splines deformation grids.
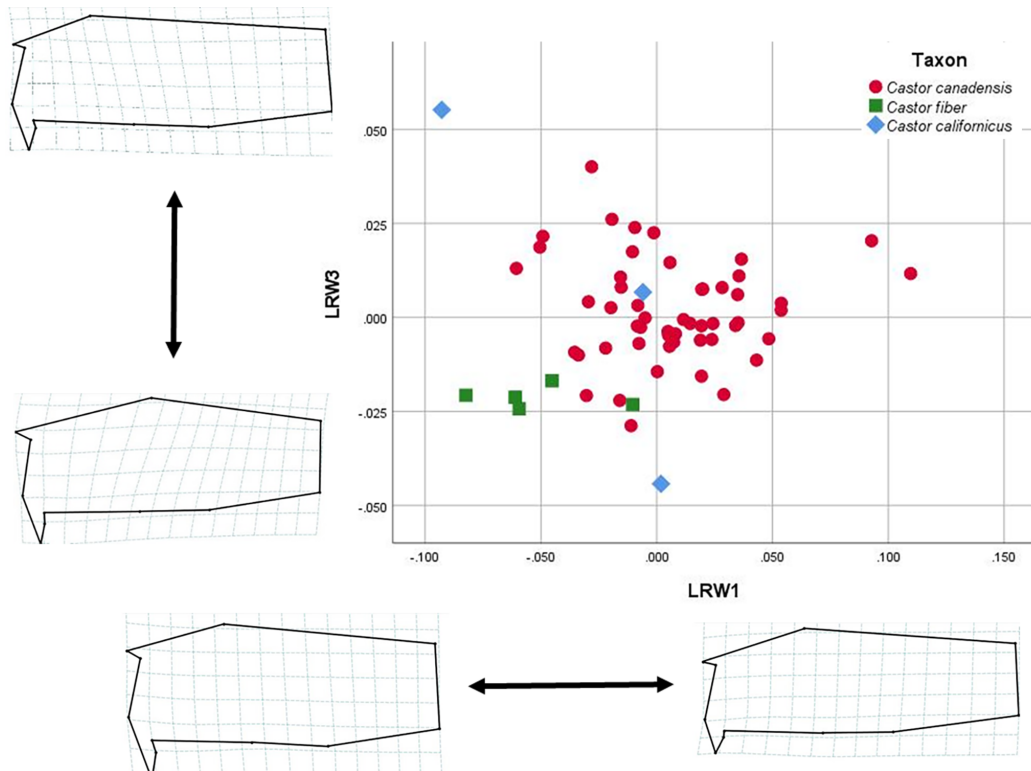

FIGURE 4. Relative warp plot for the lateral view of the cranium. Axes depict shape variation, associated with landmark deformations, indicated by thin plate splines deformation grids.

TABLE 4. Significant relative warps (Eigenvalues>1) and variance percentage attributed to shape deformation for ventral relative warps.

Relative Warp	Variance
1	29.03%
2	20.25%
3	11.08%
4	9.36%
5	7.58%
6	6.21%

and 2 showed clear separation of groups within morphospace (Figure 5). Dentary relative warp 1 (DenRW1) explained 27.71% of the variation, with *Castor fiber* clustering in positive scores, *C. californicus* in negative and low positive scores, and *C. canadensis* spanning both positive and negative scores. Negative DenRW1 scores are associated with a posterior placement of the anterior margin of the pterygoid insertion as well as larger coronoid

and angular processes. Positive DenRW1 scores are associated with the anterior placement of the anterior margin of the pterygoid insertion as well as smaller coronoid and angular processes. DenRW2 explained 14.62% of the variation, with *C. fiber* displaying negative scores, *C. californicus* positive scores, and *C. canadensis* both negative and positive scores clustering around zero. Positive DenRW2 scores are associated with a widened area between the mandibular condyle and angular process, a posterior widening of the ascending ramus (from the coronoid process to the angular process), and an elevated anteroventral border of the incisor alveolus. Negative DenRW2 scores are associated with a narrowed area between the mandibular condyle and angular process, a posterior constriction of the ascending ramus (between the coronoid process to the angular process), and a ventrally depressed anteroventral border of the incisor alveolus.
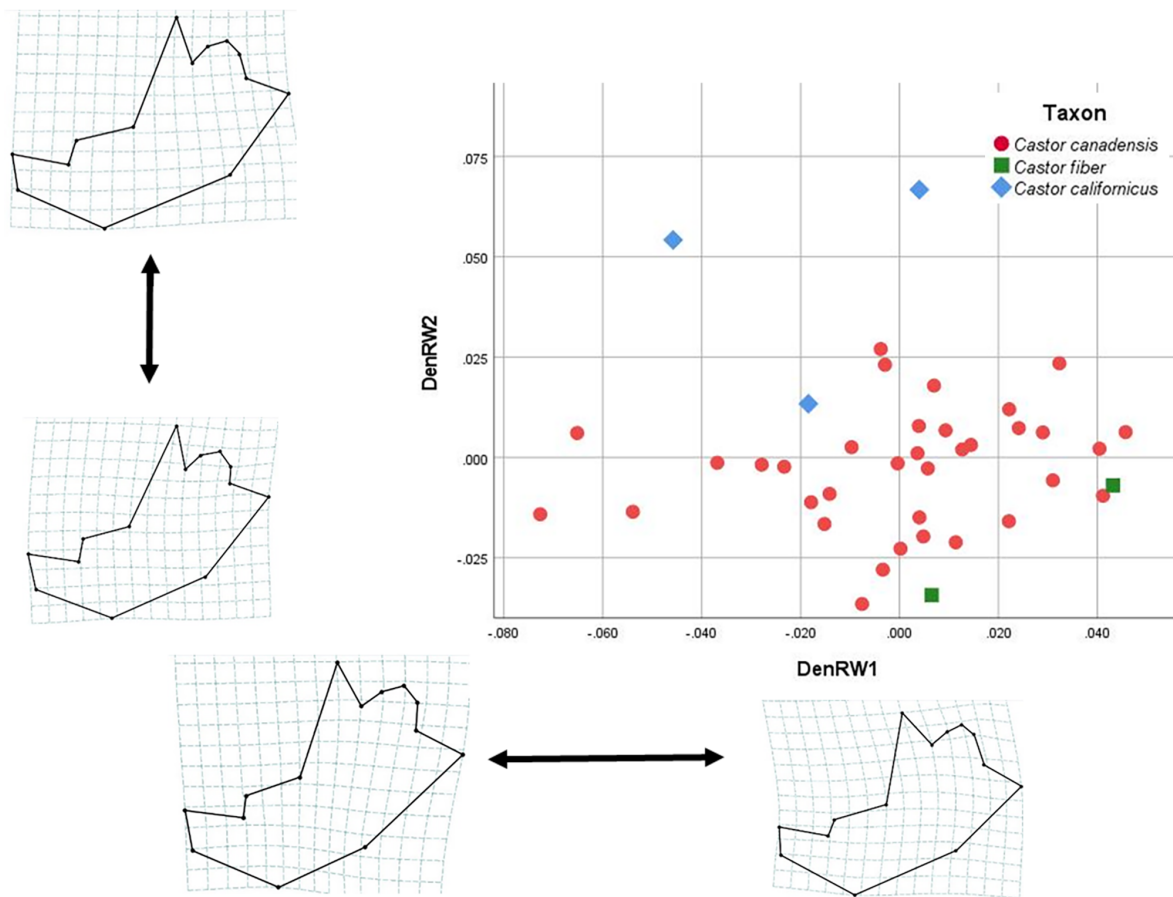

FIGURE 5. Relative warp plot for the dentary. Axes depict shape variation, associated with landmark deformations indicated by thin plate splines deformation grids.

TABLE 5. Summary statistics for cranial Canonical Variate Analysis with *Castor californicus* uncategorized.

	CV1
Eigenvalue	4.766
% Variance Explained	100
Wilk's Lambda	0.173
Chi Squared (X^2)	86.724
Canonical Correlation	0.909

Overall, *Castor fiber* and *C. canadensis* showed minimal overlap within the relative warp analyses. *Castor californicus* plotted either within or near the range of *C. canadensis* and consistently fell outside of the plotted range for *C. fiber* in morphospace.

Stepwise canonical variate analyses. The first cranial stepwise model, with *Castor californicus* categorized as unknown, included nine of the 21 partial warps and showed good separation of groups (Wilk's lambda = 0.173, $F_{(1,56)}$ = 24.360, p < 0.001). The analysis yielded one canonical variate which accounted for 100% of the variance in the dataset (Table 5). Canonical variate 1 (CV1) showed separation of *C. fiber* with high negative scores and *C. canadensis* with both positive and negative scores distributed around 0, whereas *C. californicus* had lower negative scores (Figure 6). Positive CV1 scores are associated with shorter nasals, posteromedial position of the orbit, and wider occiput.

The second cranial stepwise model, with all specimens categorized a priori, included 11 of the
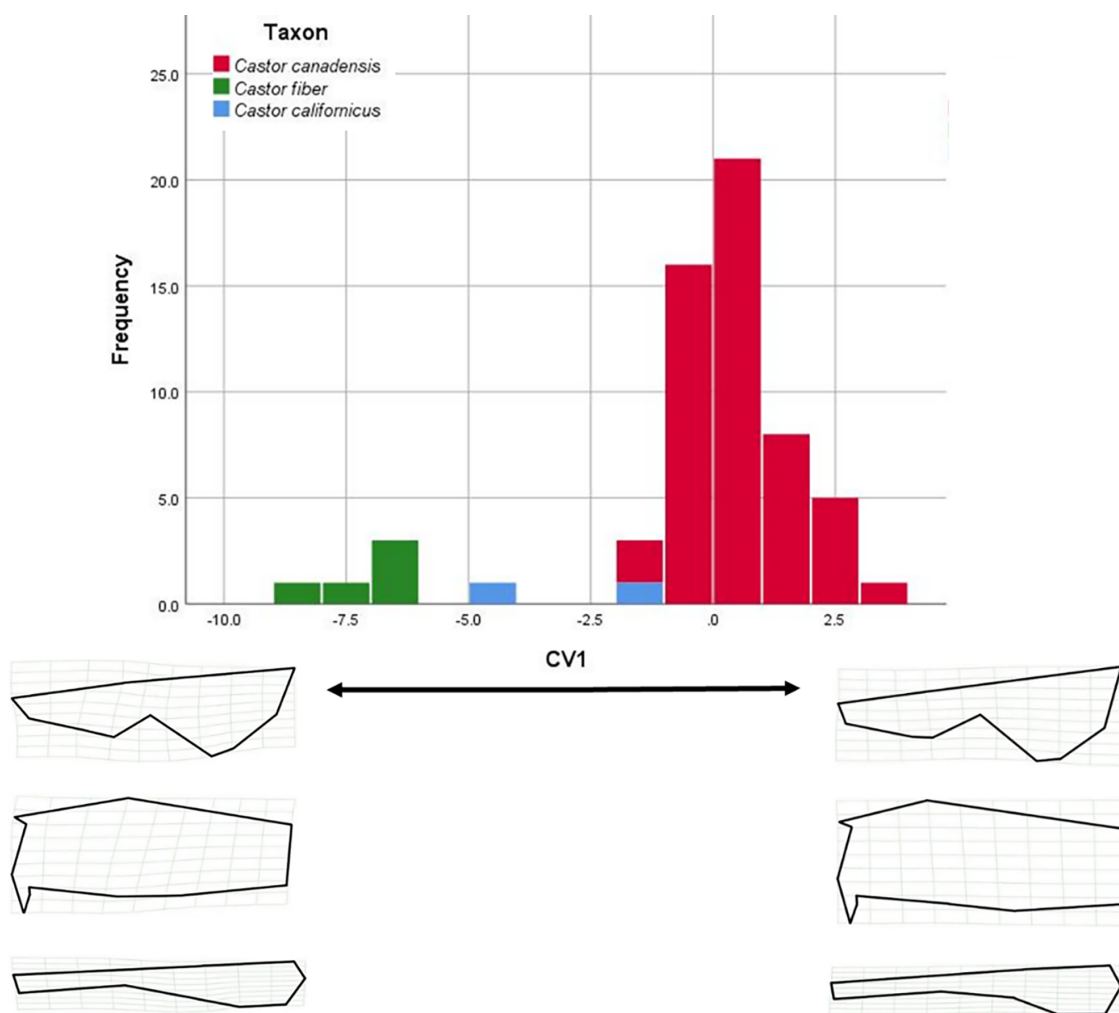

FIGURE 6. Histogram of canonical variate scores for analysis of cranial data with *Castor californicus* treated as an unknown. The x axis depicts shape variation, associated with landmark deformations, indicated by thin plate splines deformation grids. The y axis indicates the frequency of canonical variate scores among studied taxa.

TABLE 6. Summary statistics for cranial Canonical Variate Analysis with all species categorized a priori.

	CV1	CV2
Eigenvalue	4.221	2.421
% Variance Explained	63.5	36.5
Wilk's Lambda	0.056	0.292
Chi Squared (X^2)	144.131	61.501
Canonical Correlation	0.899	0.841

21 partial warps and showed significant separation of groups (Wilk's lambda 0.056, $F_{(1,56)}$ = 13.198, p < 0.001). This analysis yielded two canonical variates, which accounted for 100% of the variance in the dataset (Table 6). CV1 accounted for 63.5% of the variance and showed good separation of taxa (Figure 7); *Castor fiber* and *C. californicus* both had positive CV1 scores, whereas *C. canadensis* clustered around 0, with both positive and negative scores. Negative CV1 scores are associated with shorter nasals, wider occiput, and wider premaxillae. CV2 accounted for 36.5% of the variance and additionally showed good separation of species; *Castor fiber* had negative scores, *C. californicus* had high positive scores, and *C. canadensis* had scores close to 0, with some in both positive and negative scores. Positive CV2 scores associated are with shorter nasals and wider occiput.

The dentary stepwise model, which initially had *Castor californicus* categorized as unknowns, included six of the 11 partial warps and showed some separation of groups (Wilk's lambda = 0.351, $F_{(1, 40)}$ = 9.246, p < 0.00). The analysis yielded one canonical variate, which accounted for 100% of the variance in the dataset (Table 7). CV1 showed good separation of groups (Figure 8); *Castor fiber* had high positive scores, *C. californicus* overlapped with *C. canadensis*, but only as negative and near 0 scores, and *C. canadensis* cen-
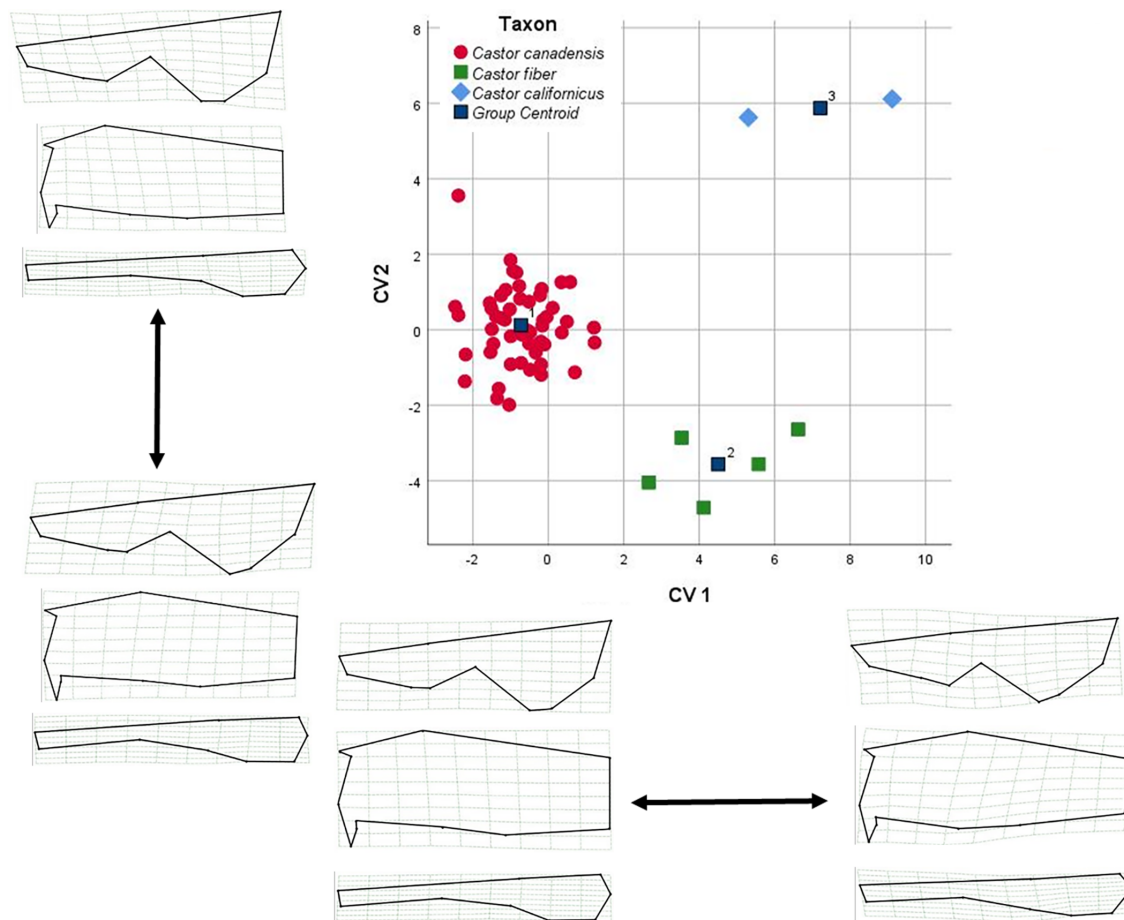

FIGURE 7. Canonical variate plot for analysis of cranial data with *Castor californicus* treated as a distinct taxon a priori. Axes depict shape variation, associated with landmark deformations, indicated by thin plate splines deformation grids.

TABLE 7. Summary statistics for dentary Canonical Variate Analysis with *Castor californicus* uncategorized

	CV1
Eigenvalue	1.849
% Variance Explained	100
Wilk's Lambda	0.351
Chi Squared (X^2)	33.504
Canonical Correlation	0.806

tered just negative of zero and contained positive and negative scores. Negative CV1 scores are associated with anterior positioned anterior margin of angular process, more obtuse curvature between coronoid and condylar processes, and anteriorly oriented coronoid process.

The second dentary stepwise model, with all species categorized a priori, included three of the 11 partial warps and showed significant separation of groups (Wilk's lambda = 0.329, $F_{(2,40)}$ = 8.658, *p* < 0.00). This analysis yielded two canonical variates, which accounted for 100% of the variance in the dataset (Table 8). CV1 accounted for 80.5% of the variance and showed separation of *Castor californicus* with negative scores from *C. fiber* with positive scores, and *C. canadensis* with scores centered around 0, with some spread into positive and negative scores (Figure 9). Positive CV1 scores are associated with posterior positioning of coronoid process, shorter condylar process, dorsal
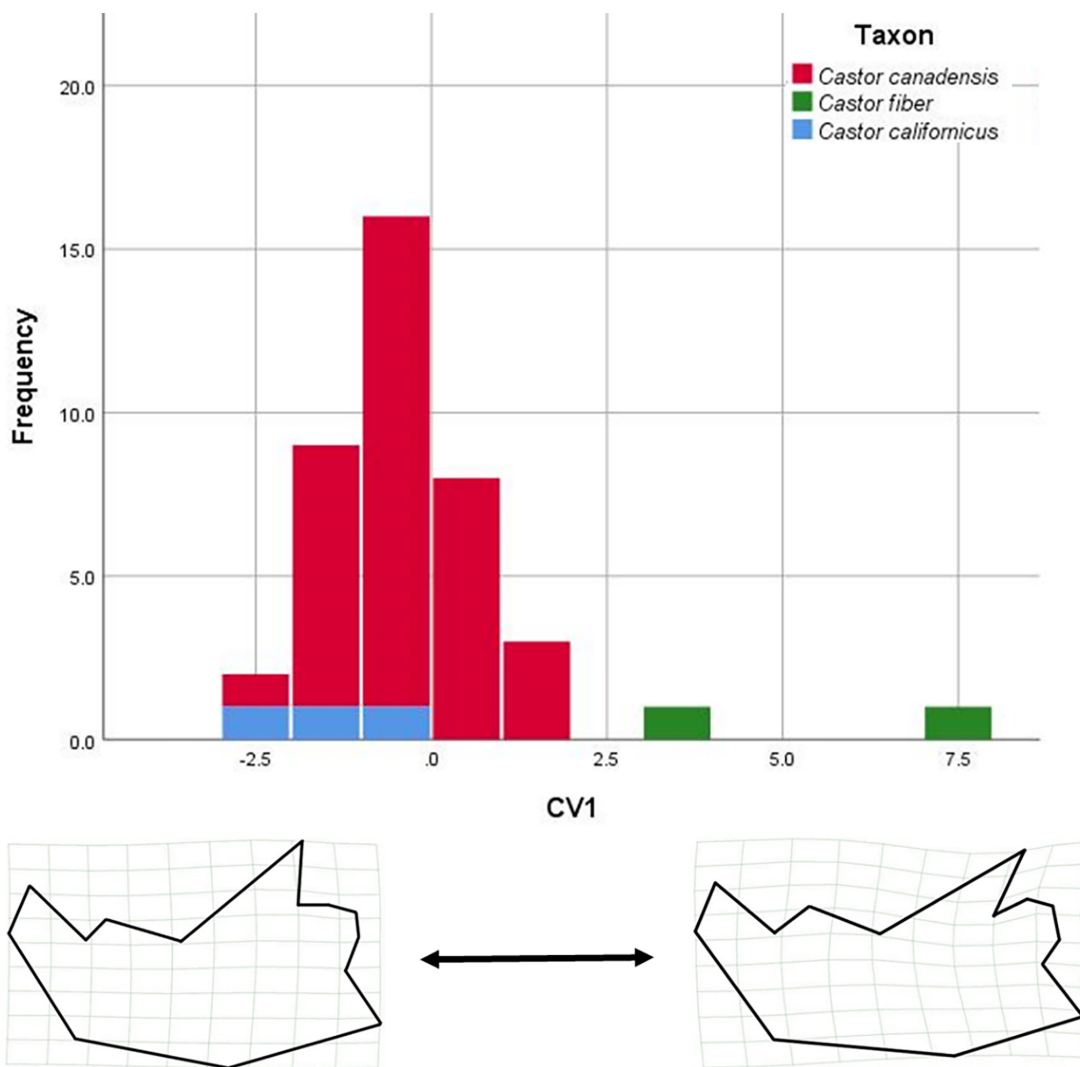

FIGURE 8. Histogram of canonical variate scores for analysis of dentary data with *Castor californicus* treated as an unknown. The x axis depicts shape variation, associated with landmark deformations, indicated by thin plate splines deformation grids. The y axis indicates the frequency of canonical variate scores among studied taxa.

TABLE 8. Summary statistics for dentary Canonical Variate Analysis with all species categorized a priori

	CV1	CV2
Eigenvalue	1.307	0.316
% Variance Explained	80.5	19.5
Wilk's Lambda	0.329	0.760
Chi Squared (X^2)	39.968	9.876
Canonical Correlation	0.753	0.490

positioning of angular process, and anteriorly extended ascending ramus. CV2 accounted for 19.5% of the variance and showed some separation of groups, *C. californicus* had positive scores and near 0 values, *C. fiber* had highly positive values, and *C. canadensis* clustered near 0 in both positive and negative scores. Positive CV2 scores associated with posterior positioning of the ascending ramus, ventral expansion of the angular process, and anteriorly oriented coronoid process.

The first cranial CVA classification resulted in 100% correct classification of individuals with 98.3% correct classification when cross-validated (Table 9). One specimen of *Castor canadensis* (MVZ 183809) was misclassified as *C. fiber* in cross-validation. *Castor californicus*, which was assigned as unknown for this cranial CVA, included specimens classified as both *C. fiber* and *C. californicus*. Those classifications had low conditional probabilities, which suggests low likelihood of those fossil specimens belonging to those species (Table 10).

The second cranial CVA classification, in which all species were assigned a priori, resulted in 100% correct classification of individuals with 98.3% correct classification when cross validated (Table 11). One specimen of *Castor californicus* (UF 225200) was classified as *C. canadensis* in cross-validation. The classification of that specimen had a low conditional probability, which sug-
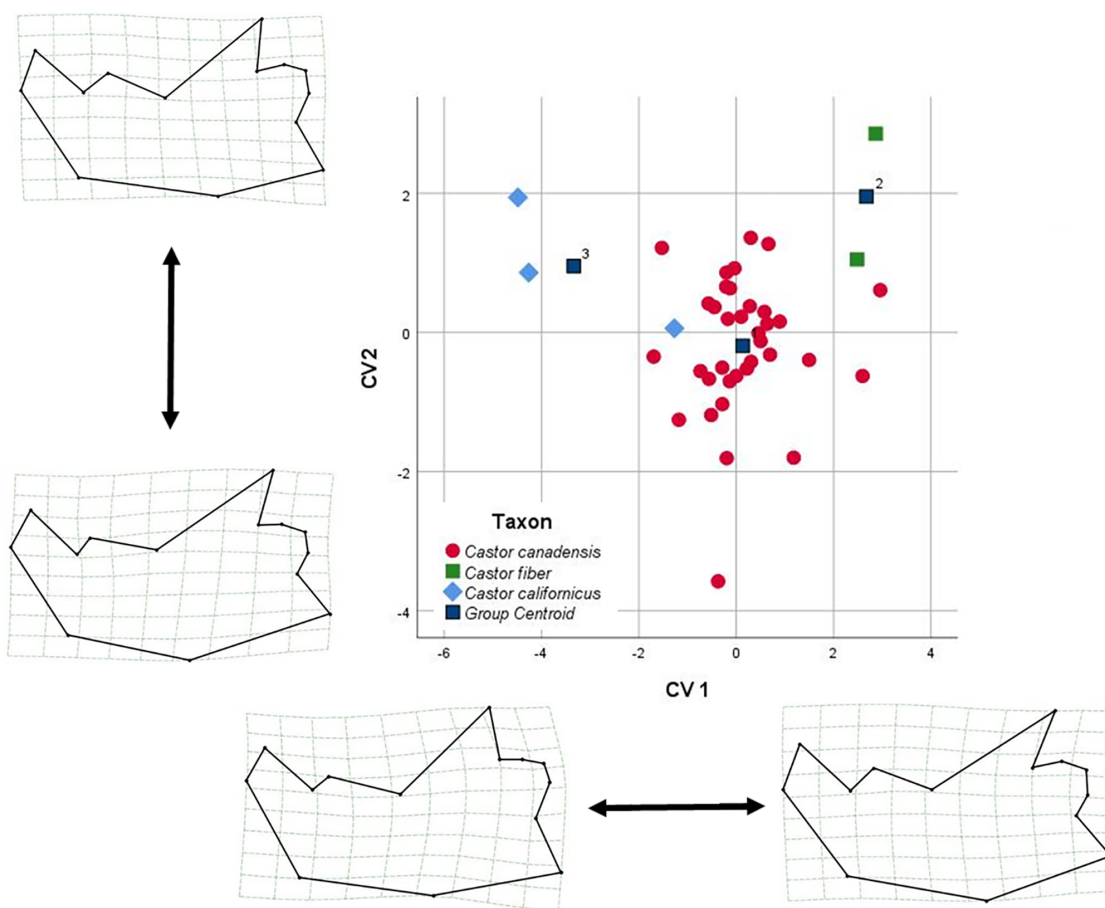

FIGURE 9. Canonical variate plot for analysis of dentary data with *Castor californicus* treated as a distinct taxon a priori. Axes depict shape variation, associated with landmark deformations, indicated by thin plate splines deformation grids.

TABLE 9. Cranial CVA classification matrix with *Castor californicus* uncategorized

	Taxon	*Castor canadensis*	*Castor fiber*	Total
Original	C. canadensis	53	0	53
	C. fiber	0	5	5
	C. californicus	1	1	2
Cross-validated	C. canadensis	52	1	53
	C. fiber	0	5	5

TABLE 10. Cranial CVA classifications with *Castor californicus* uncategorized. P(D/G) represents the conditional probability of the canonical score given most likely group membership. P(G/D) represents the posterior probability that a specimen belongs to the predicted group, based on the original group assignment.

Specimen	Most Likely Group	P(D/G)	P(G/D)	2nd Most Likely Group
C. californicus (UF225200)	C. canadensis	0.060	1.000	C. fiber
C. californicus (USNM26154)	C. fiber	0.005	0.994	C. canadensis

TABLE 11. Cranial CVA classification matrix with all species categorized a priori.

	Taxon	*Castor canadensis*	*Castor fiber*	*Castor californicus*	Total
Original	C. canadensis	51	0	0	51
	C. fiber	0	5	0	5
	C. californicus	0	0	2	2
Cross-validated	C. canadensis	51	0	0	51
	C. fiber	0	5	0	5
	C. californicus	1	0	1	2

TABLE 12. Cranial CVA classification with all species categorized a priori. P(D/G) represents the conditional probability of the canonical score given most likely group membership. P(G/D) represents the posterior probability that a specimen belongs to the predicted group, based on the original group assignment.

Specimen	Most Likely Group	P(D/G)	P(G/D)	2nd Most Likely Group
C. californicus (UF225200)	C. canadensis	0.000	1.000	C. fiber

TABLE 13. Dentary CVA classification matrix with *Castor californicus* uncategorized.

	Taxon	*Castor canadensis*	*Castor fiber*	Total
Original	C. canadensis	35	0	35
	C. fiber	0	2	2
	C. californicus	3	0	3
Cross-validated	C. canadensis	35	0	35
	C. fiber	1	1	2

gests low likelihood of belonging to *C. canadensis* (Table 12).

Dentary CVA classification, where *Castor californicus* was assigned as unknown, resulted in 100% correct classification of individuals with 97.3% correct classification when cross-validation

(Table 13). *Castor californicus* specimens were classified as *C. canadensis* and one specimen of *C. fiber* (USNM 174938) was misclassified as *C. canadensis* in cross-validation. Conditional probabilities for *C. californicus* indicate those specimens

TABLE 14. Dentary CVA classification with *Castor californicus* uncategorized. P(D/G) represents the conditional probability of the canonical score given most likely group membership. P(G/D) represents the posterior probability that a specimen belongs to the predicted group, based on the original group assignment.

Specimen	Most Likely Group	P(D/G)	P(G/D)	2nd Most Likely Group
C. californicus (USNM26154)	*C. canadensis*	0.015	1.000	*C. fiber*
C. californicus (UF225200)	*C. canadensis*	0.820	1.000	*C. fiber*
C. californicus (UOMNCH16338)	*C. canadensis*	0.322	1.000	*C. fiber*

TABLE 15. Dentary CVA classification matrix with all species categorized a priori.

	Taxon	*Castor canadensis*	*Castor fiber*	*Castor californicus*	Total
Original	*C. canadensis*	34	1	0	35
	C. fiber	0	2	0	2
	C. californicus	1	0	2	3
Cross-validated	*C. canadensis*	34	1	0	35
	C. fiber	1	1	0	2
	C. californicus	1	0	2	3

TABLE 16. Dentary CVA classification with all species categorized a priori. P(D/G) represents the conditional probability of the canonical score given most likely group membership. P(G/D) represents the posterior probability that a specimen belongs to the predicted group, based on the original group assignment.

Specimen	Most Likely Group	P(D/G)	P(G/D)	2nd Most Likely Group
C. californicus (USNM26154)	*C. canadensis*	0.363	0.982	*C. californicus*

fall within the range of variation for *C. canadensis* (Table 14).

Dentary CVA classification in which all species were assigned a priori resulted in 95% correct classification of individuals with 92.5% correct classification when cross-validated (Table 15). In this analysis, some specimens were misclassified between groups. One specimen of *Castor canadensis* (LACM 93330) was classified as *C. fiber* in both the original classification and cross validation. One specimen of *C. fiber* (USNM 174938) was misclassified as *C. canadensis* in cross validation and one specimen of *C. californicus* (USNM 26154) was classified as *C. canadensis*. Conditional probabilities indicate those specimens fall within the range of variation for the assigned species (Table 16).

Cluster analysis. The cluster analysis of cranial data resulted in some separation between species (Figure 10). All *Castor fiber* specimens grouped together, except for one specimen (MVZ 19229), which clustered with *C. canadensis.* This specimen consistently clustered separately from the other *C. fiber* specimens, as shown in the relative warp graphs produced from the RWA. This separation

could be attributed to MVZ 19229 having distinct morphological differences compared to the other *C. fiber* specimens included in the analysis, including an elongated rostrum, narrow zygomatic arches, and widened posterior cranium.

Nearly all North American *Castor* specimens grouped together, with *C. californicus* nested within the *C. canadensis* cluster (Figure 10). *Castor fiber* specimens clustered together, except for MVZ 19229, which grouped apart from other specimens of the species in other analyses. An outgroup, formed by three specimens, formed outside of the *C. canadensis* and *C. fiber* clusters. Those specimens included two *C. canadensis* (MVZ 80744 and UCLA 9517) and one *C. californicus* (USNM 26154). Uniform components and partial warp scores of those three outlier specimens showed no clear indication of similarities or extreme variation in scores which might separate those specimens from the other *C. canadensis* group.

The cluster analysis of dentary data resulted in two prominent groupings (Figure 11). All *Castor canadensis* grouped together, with *C. fiber* specimens (USNM 174938 and USNM 248154) grouped within *C. canadensis* specimens. An early Pleisto-
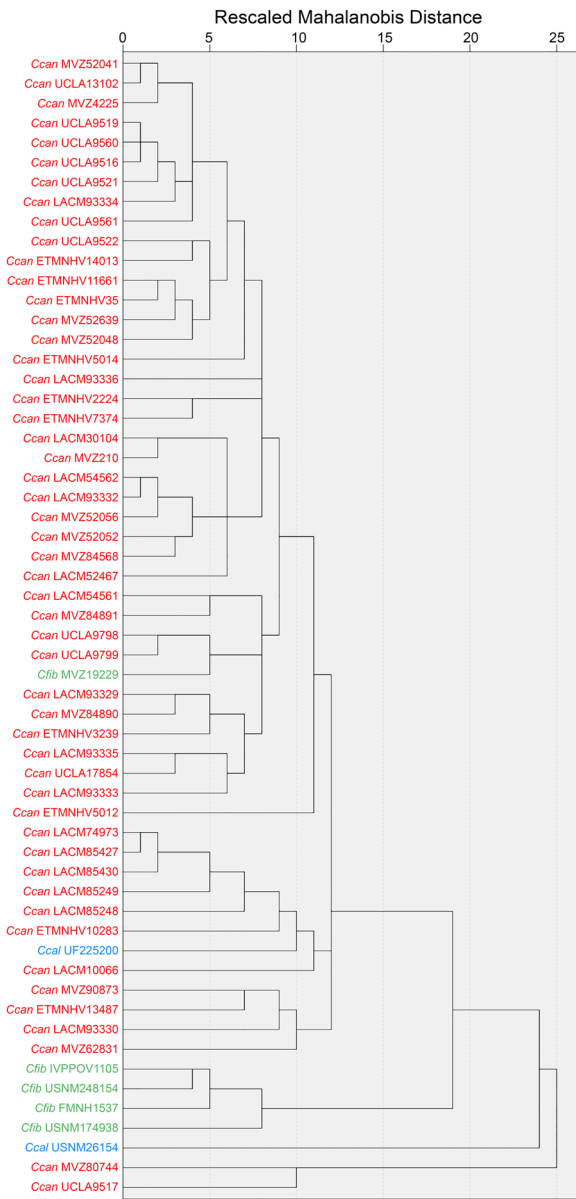
FIGURE 10. Dendrogram of cranial hierarchical cluster analysis. Specimens used in analysis are labeled by species and catalog number.
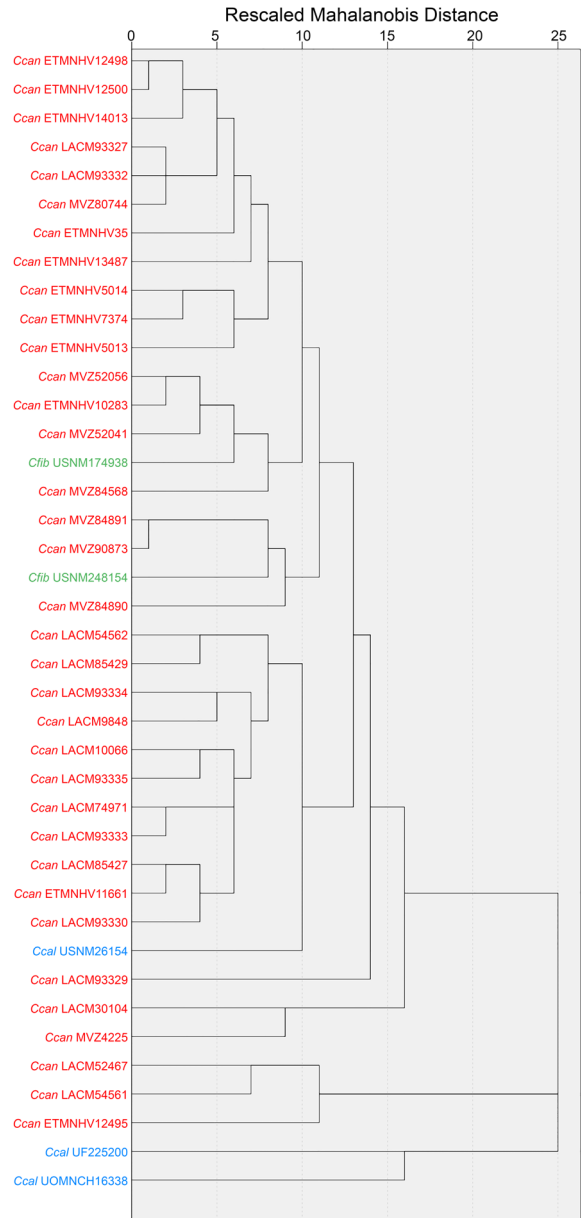

FIGURE 11. Dendrogram of dentary hierarchical cluster analysis. Specimens used in analysis are labeled by species and catalog number.

cene aged *C. californicus* (and a specimen previously referred to *C. accessor*) clustered together, forming the outgroup from the extant species.

Postcranial Analysis

Descriptive statistics and ANOVA. *Castor californicus* had significantly larger mean values than *C. canadensis* for most variables in this analysis (Table 17). Maximum and minimum range values show *C. californicus* has substantial overlap in size when compared to *C. canadensis.* Comparisons to *C. fiber* were limited due to inadequate sampling.

Postcranial elements with little overlap in range values include FeAPD and TDEMLD (Figure 12). *Castor californicus* had a broad femur anteroposterior diameter (FeAPD) compared to *C. canadensis. Castor californicus* also has a wider mediolateral diameter on the distal end of the tibia (TDEMLD) than *C. canadensis*.

Castor californicus and *C. canadensis* do not overlap in several measurements (Figure 13). *Castor californicus* has a wider humeral distal articular width (HDAW), greater anteroposterior diameter of

TABLE 17. Descriptive statistics, coefficients of variation with sample size correction (CV*) (following Sokal and Brau-mann, 1980), and ANOVA results for species postcranial measurements (N ≤ 3). Statistically significant *p*-values bolded for clarity. (Continued on next page.)

Measurement	Taxon	N	Mean (μ)	St. Dev (σ)	Min	Max	CV*(%)	F (df)	p
HMLD	*C. can*	22	10.75	0.76	9.55	12.00	7.18	14.199 (2)	**0.000**
	C. fib	1	7.49	-	7.49	7.49	-		
	C. cal	3	12.31	1.06	11.27	13.38	9.29		
HDAW	*C. can*	21	19.85	0.80	18.18	21.22	4.08	26.849 (1)	**0.000**
	C. fib	0	-	-	-	-	-		
	C. cal	4	22.01	0.44	21.64	22.62	2.12		
UL	*C. can*	20	119.66	4.01	112.99	130.28	3.39	29.586 (2)	**0.000**
	C. fib	1	85.07	-	85.07	85.07	-		
	C. cal	3	124.47	8.32	115.01	130.64	7.24		
ULOL	*C. can*	20	25.23	1.68	22.28	28.57	6.74	14.801 (2)	**0.00**
	C. fib	1	16.29	-	16.29	16.29	-		
	C. cal	3	23.91	0.98	23.30	25.04	4.44		
FeL	*C. can*	24	99.75	5.59	89.44	110.81	5.66	20.802 (2)	**0.000**
	C. fib	2	77.93	12.52	69.08	86.78	-		
	C. cal	6	109.82	6.45	98.70	117.27	6.12		
FeAPD	*C. can*	24	11.78	1.03	9.93	13.40	8.82	12.334 (3)	**0.000**
	C. fib	2	10.60	2.49	8.84	12.36	-		
	C. cal	8	14.08	0.86	13.21	15.60	6.28		
FeMLD	*C. can*	24	24.94	1.52	21.18	27.94	6.14	2.694 (3)	0.063
	C. fib	2	21.78	7.75	16.30	27.26	-		
	C. cal	9	26.56	2.55	23.13	31.05	9.88		
FeGT	*C. can*	23	13.17	1.99	10.27	18.07	15.24	4.071 (1)	0.054
	C. fib	0	-	-	-	-	-		
	C. cal	6	15.29	3.31	11.98	19.36	22.56		
FeHD	*C. can*	21	17.16	0.65	16.10	19.22	3.86	64.657 (1)	**0.000**
	C. fib	0	-	-	-	-	-		
	C. cal	6	20.20	1.27	18.15	21.55	6.53		
FeEB	*C. can*	22	34.13	1.81	30.44	37.10	5.38	58.219 (1)	**0.000**
	C. fib	0	-	-	-	-	-		
	C. cal	5	41.72	2.81	39.79	46.57	7.08		
TL	*C. can*	19	131.29	5.23	119.75	142.91	4.04	12.805 (1)	**0.002**
	C. fib	0	-	-	-	-	-		
	C. cal	3	145.75	13.28	131.08	156.97	9.87		
TAPD	*C. can*	19	14.64	1.62	11.02	17.03	11.05	0.76 (1)	0.39
	C. fib	0	-	-	-	-	-		
	C. cal	4	13.89	1.19	12.40	15.24	8.59		
TMLD	*C. can*	19	12.97	1.20	10.74	15.67	9.41	8.379 (1)	**0.009**
	C. fib	0	-	-	-	-	-		
	C. cal	4	15.12	2.00	13.28	17.41	14.04		
TPEMLD	*C. can*	18	32.61	1.24	30.94	35.50	3.86	12.258 (1)	**0.002**
	C. fib	0	-	-	-	-	-		
	C. cal	3	36.23	3.61	32.14	38.99	10.80		

TABLE 17 (continued from previous page).

Measurement	Taxon	N	Mean (μ)	St. Dev (σ)	Min	Max	CV*(%)	F (df)	p
TDEAPD	*C. can*	18	16.34	0.75	15.17	17.78	4.65	27.859 (1)	***0.000***
	C. fib	0	-	-	-	-	-		
	C. cal	4	18.38	0.23	18.20	18.69	1.33		
TDEMLD	*C. can*	18	19.08	1.03	16.92	20.67	5.45	21.194 (1)	***0.000***
	C. fib	0	-	-	-	-	-		
	C. cal	5	21.88	1.78	20.17	24.53	8.52		
TLOF	*C. can*	18	39.98	3.56	33.94	45.48	9.02	1.092 (1)	0.309
	C. fib	0	-	-	-	-	-		
	C. cal	3	37.56	4.81	33.18	42.71	13.87		
MT3L	*C. can*	16	49.04	3.46	45.35	59.76	7.16	3.584 (1)	0.075
	C. fib	0	-	-	-	-	-		
	C. cal	3	53.22	3.88	49.03	56.70	7.90		
MT3APD	*C. can*	8	6.20	0.34	5.66	6.71	5.65	25.608 (1)	***0.000***
	C. fib	0	-	-	-	-	-		
	C. cal	5	7.90	0.87	7.09	9.35	11.56		
MT3MLD	*C. can*	8	7.58	0.53	6.65	8.16	7.20	10.312 (1)	***0.008***
	C. fib	0	-	-	-	-	-		
	C. cal	5	9.06	1.15	7.25	9.95	13.29		
MT4L	*C. can*	13	56.73	2.23	52.76	60.78	4.01	12.030 (1)	***0.003***
	C. fib	0	-	-	-	-	-		
	C. cal	4	61.22	2.39	58.08	63.52	4.15		
MT4APD	*C. can*	6	7.59	0.18	7.33	7.85	2.46	0.134 (1)	0.721
	C. fib	0	-	-	-	-	-		
	C. cal	8	7.72	0.85	6.77	9.00	11.29		
MT4MLD	*C. can*	6	8.64	0.25	8.38	9.05	2.99	63.129 (1)	***0.000***
	C. fib	0	-	-	-	-	-		
	C. cal	8	10.57	0.55	9.87	11.40	5.36		
MT5L	*C. can*	14	41.23	2.93	33.81	46.28	7.22	5.137 (1)	***0.039***
	C. fib	0	-	-	-	-	-		
	C. cal	3	45.33	2.21	43.04	47.45	5.28		
MT5APD	*C. can*	7	5.76	0.28	5.54	6.26	5.09	9.642 (1)	***0.015***
	C. fib	0	-	-	-	-	-		
	C. cal	3	6.61	0.62	5.96	7.19	10.13		
MT5MLD	*C. can*	7	5.53	0.43	4.83	6.07	8.12	5.407 (1)	***0.049***
	C. fib	0	-	-	-	-	-		
	C. cal	3	6.25	0.49	5.69	6.60	8.46		

the third metatarsal (MT3APD), and greater medio-lateral diameter of the fourth metatarsal (MT4MLD) than *C. canadensis*. *Castor californicus* also has an anteroposteriorly broader distal end of the tibia (TDEAPD) and greater femoral epicondylar breadth (FeEB) than *C. canadensis.*

Coefficients of variation. Coefficients of variation were calculated for measurements with more than three samples per species, which were sample size corrected included with descriptive statistics and ANOVA results (Table 17). Species overall showed high levels of variation within postcranial elements (Figure 14).
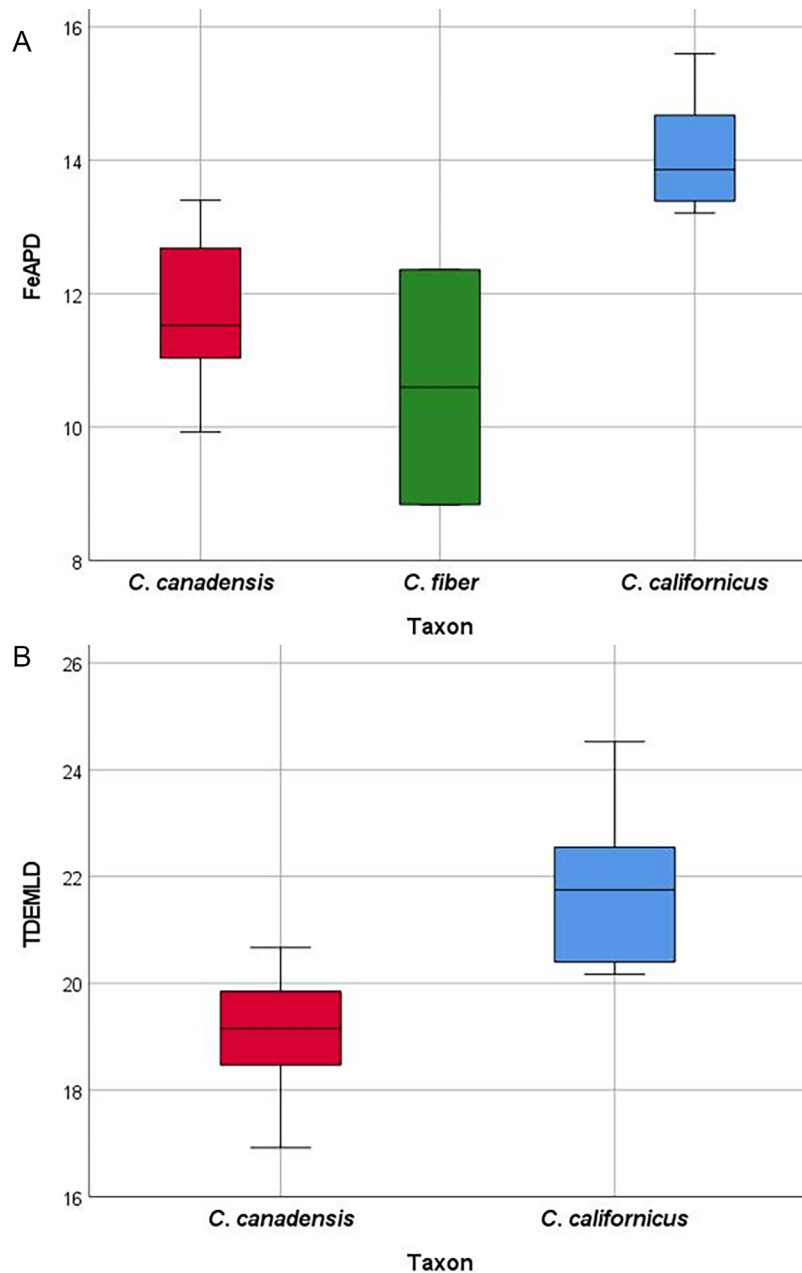
FIGURE 12. Boxplots for (A) anteroposterior diameter of femur (FeAPD) and (B) mediolateral diameter of tibia distal epiphysis (TDEMLD) of *Castor canadensis* and *C. californicus*, which exhibit differences in mean values and minimal overlap in range values. See Table 17 for descriptive statistics, coefficients of variation, and ANOVA results.

DISCUSSION AND CONCLUSIONS

The earliest occurrence of the genus *Castor* in North America is from the late Miocene, as represented by *Castor californicus* (Samuels and Zancanella, 2011). Although previously described as a different species from the extant North American beaver *C. canadensis*, morphological similarities between Miocene to early Pleistocene-aged fossil and extant North American beavers warrant a re-evaluation of the fossil taxa to determine if *C. californicus* is distinct from *C. canadensis*. Here we present a morphological evaluation between the Miocene to early Pleistocene-aged *C. californicus* and the late Pleistocene-aged and extant *C. canadensis*.
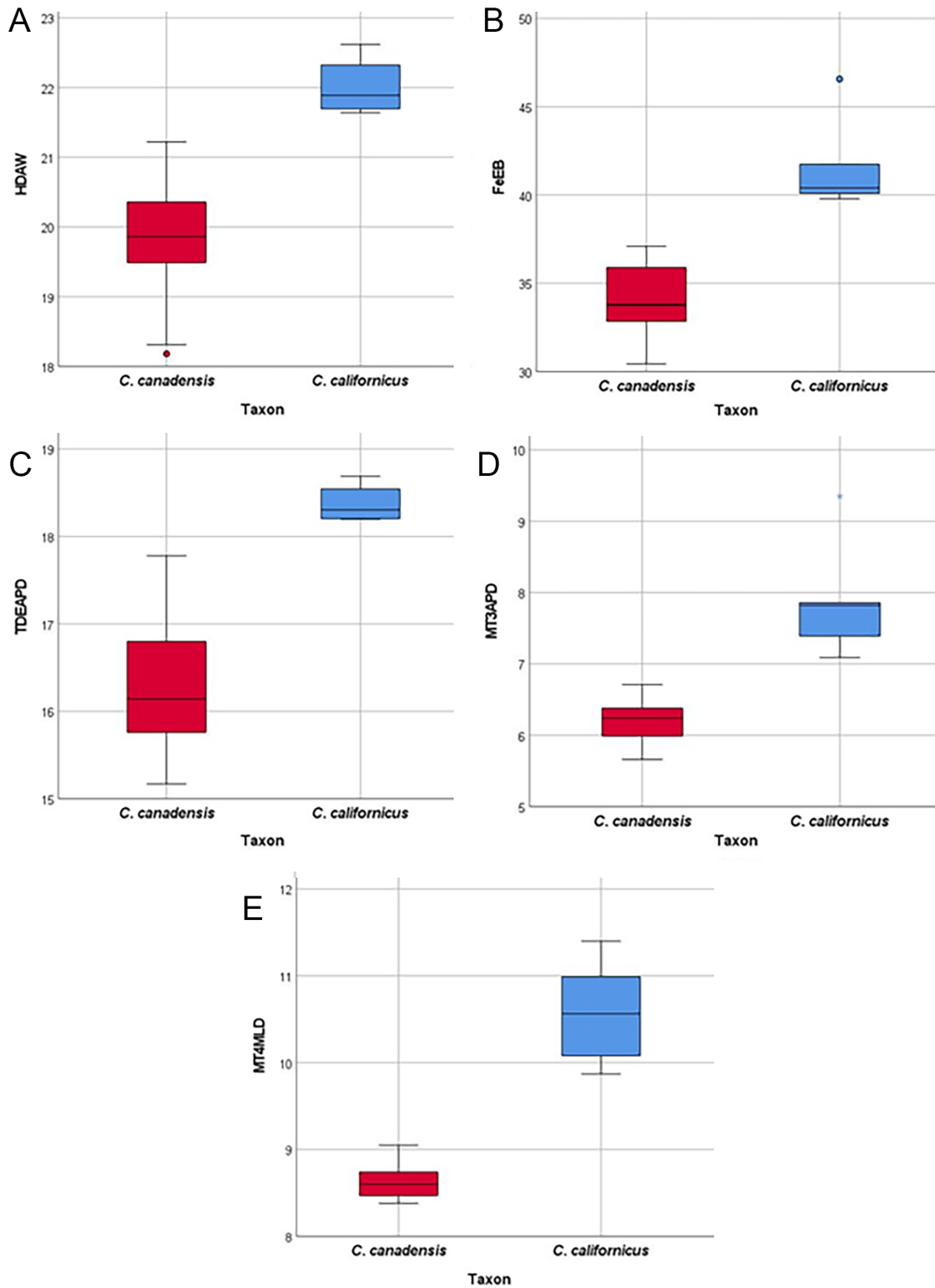
FIGURE 13. Boxplots for (A) articular width of humeral distal end (HDAW), (B) femoral epicondylar breadth (FeEB), (C) anteroposterior diameter of tibia distal epiphysis (TDEAPD), (D) anteroposterior diameter of third metatarsal (MT3APD), and (E) mediolateral diameter of fourth metatarsal (MT4MLD) of *Castor canadensis* and *C. californicus,* which exhibit differences in mean values and no overlap in range values. See Table 17 for descriptive statistics, coefficients of variation, and ANOVA results.
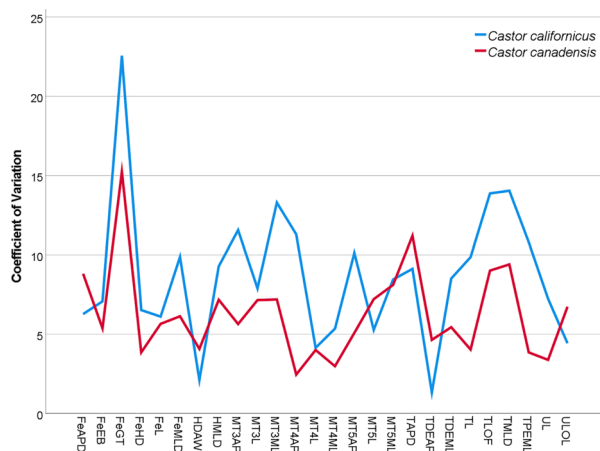
FIGURE 14. Variation line graph calculated by coefficients of variation with sample size correction for *Castor canadensis* and *C. californicus* postcranial measurements. Note that *C. fiber* is excluded due to limited sampling. *Castor canadensis* and *C. californicus* both contains high levels of variation in postcranial elements. See Table 17 for descriptive statistics, coefficients of variation, and ANOVA results.

Morphological Similarities

Castor canadensis shows high levels of variation in skull morphology. The geometric morphometric analysis all resulted in widespread distribution of the species within morphospace. It has been noted in previous literature that *C. canadensis* is highly variable (Stefen, 2009), as at one time it was separated into subspecies based on phenotypic characteristics and regional distribution across North America (Rhoads, 1898; Jenkins and Buscher, 1979; Long, 2000). Specimens of *C. canadensis* used in this study here were collected from across North America (Appendices 1 and 2); therefore, the resulting variation seen within the species is a good representation of the variation seen across the continent in the recent past and present. Some of the variation seen in *C. canadensis* may also be partially attributed to ontogenetic changes in skull shape within older adults (greater than 5 years old) after reaching sexual maturity (Segura et al., 2023), as has been previously noted with the sagittal crest of extant beavers (Hinze, 1950). *Castor fiber* may also have similarly high morphological variability in the skull, suggested by the wide separation of MVZ 19229 from other specimens across analyses, but limited sampling here precludes rigorous evaluation of that possibility. Prior work has also documented high intraspecific variability in the dentition of both *C.*

canadensis and *C. fiber* (Stefen, 2009), with much of the variation attributable to ontogenetic changes.

Castor californicus consistently plots within the observed range of variation of *C. canadensis* across both relative warp and canonical variate analyses of the cranium (Figures 3 – 9). Within the classification stage of both the cranial and dentary CVA, *C. californicus* primarily categorized with *C. canadensis* (Tables 10 – 16). *Castor californicus* clustered within *C. canadensis* in the cranial hierarchical cluster analysis (Figure 10), indicating strong, shared morphological similarities between the two species.

This suggests cranial morphological features are more similar in *Castor canadensis* and *C. californicus* than either is with *C. fiber*. Across relative warp analyses, *C. fiber* consistently plots separate from *C. canadensis* and *C. californicus*, highlighting the distinct morphological differences between extant beaver species (Troszyński, 1975; Flynn and Jacobs, 2008; Danilov et al., 2011; Kauhala and Timonen, 2016). Previous studies on the mitochondrial DNA of *C. canadensis* and *C. fiber* show that the two species last shared a common ancestor as early as 7.5 m.y.a. (Horn et al., 2011). This timing corresponds with the oldest known record of *C. californicus* in North America from the Rattlesnake Formation in Oregon (Samuels and Zancanella, 2011).

Cranial morphological similarities between *Castor canadensis* and *C. californicus* broadly include shorter nasals, wider occiput, and posteriorly positioned orbits when compared to *C. fiber* (Figure 15). Dentaries of *C. canadensis* and *C. californicus* both display anterior placement of the anterior margin of the pterygoid insertion and greater spread of the posterior processes (coronoid, condylar, angular) (Figure 15). These findings suggest both North American species have higher mechanical advantage and potentially larger pterygoid muscles than *C. fiber*, and a broader nuchal region which represents the insertion area of the head-stabilizing neck muscles.

Studied specimens of *Castor californicus* fit largely within the wide range of morphological variation seen in *C. canadensis* postcrania (Table 17). The postcranial analysis of *C. fiber* is limited due to inadequate sampling, precluding detailed comparisons to either North American species. The postcranial elements, which were measured, did document differences from those of *C. canadensis*, though not enough data were collected to confidently evaluate morphological differences between these species.
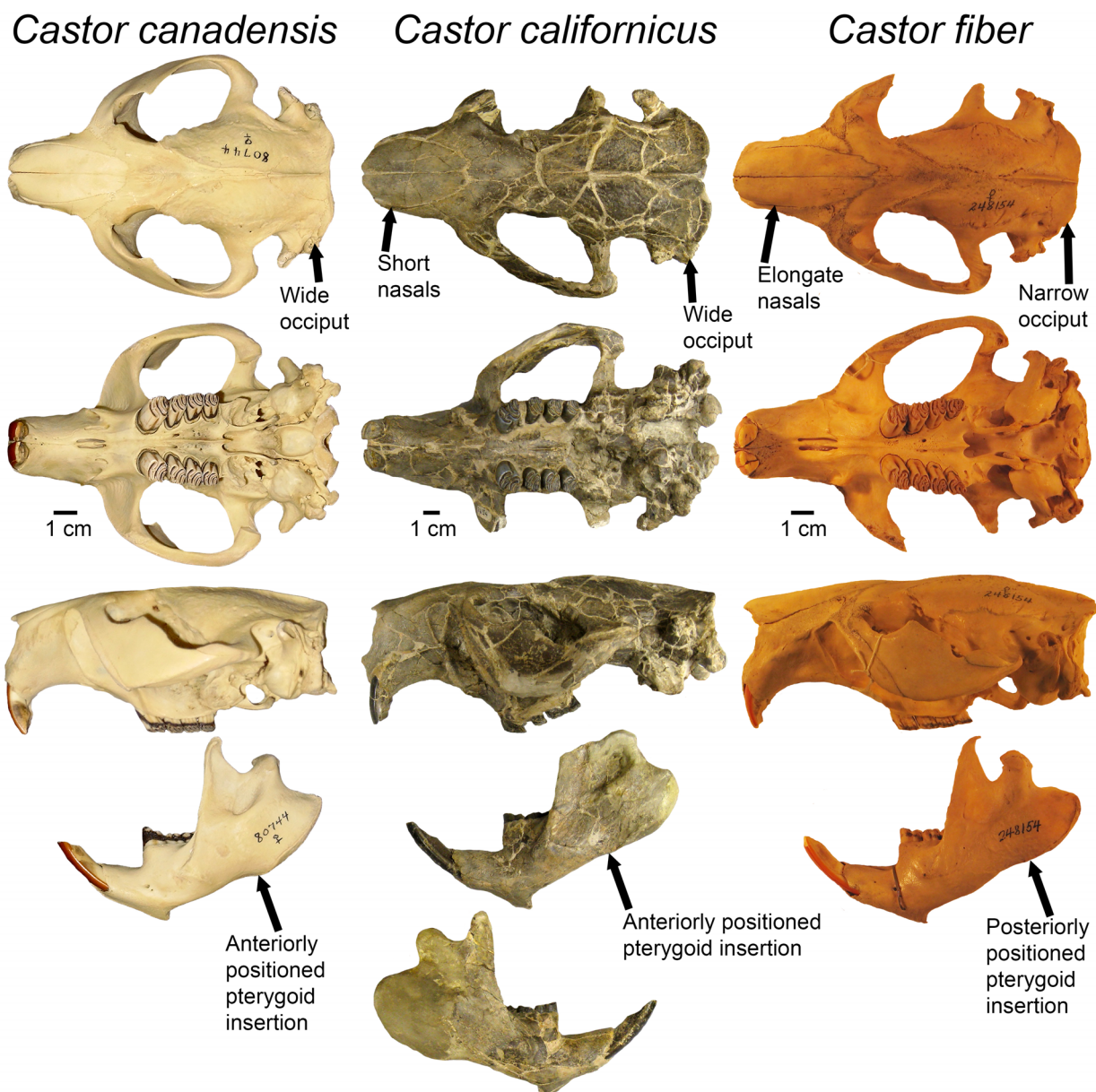
FIGURE 15. Comparison of the skull and dentary of extant *Castor canadensis* (MVZ 80744) and *C. fiber* (USNM 248154) to fossil *C. californicus* (USNM 26154). Note that the North American species *C. canadensis* and *C. californicus* share shorter nasals, wider occiput, and more posteriorly positioned orbits than Eurasian *C. fiber*; both also display more anterior placement of the anterior margin of the pterygoid insertion and greater spread of the posterior processes (coronoid, condylar, angular) than *C. fiber*.

Castor canadensis and *C. californicus* show high levels of variation in postcranial morphology, as evidenced by coefficients of variation, which were also highly variable for both species even with sample size corrections. Previous studies of *C. californicus* described it as closely resembling the extant *C. canadensis* but larger in size (Stirton, 1935; Shotwell, 1970). High intraspecific variability in both taxa and substantial overlap in measure-ments suggests that differentiating these species based on size is not reliable. Other studies have found size is not generally a reliable metric for identifying and distinguishing species (Koch, 1986; Stefen, 2010; Emery-Wetherell and Davis, 2018; Martin et al., 2018). Given the degree of morpho-logical variation observed in extant *C. canadensis* (data presented here and for dentition by Stefen, 2009), size alone should not be used to distinguish

C. californicus from *C. canadensis*. Although certain postcranial features showed differences in range between *C. californicus* and *C. canadensis*, most *C. californicus* elements measured in the study fit within the observed range of variation for *C. canadensis*.

Morphological Distinctions

Castor canadensis and *C. californicus* show some morphological distinctions within the dentary and postcrania. Most specimens of *C. californicus* fell outside of the range of *C. canadensis,* in the relative warp analysis of the dentary (Figure 5). The hierarchical cluster analysis of the dentary showed greater separation between species, with most specimens of *C. californicus* forming the outgroup from *C. canadensis* and *C. fiber* (Figure 11), reflecting morphological differences from the extant species.

Semi-aquatic rodents exhibit a wide range of osteological specializations for their lifestyles (Howell, 1930; Gingerich, 2003; Samuels and Van Valkenburgh, 2008; Calede, 2022). Postcranial characteristics include shortening of the femur, robust limb elements, enlarged muscle attachment sites for the hind limb, and elongated hindfoot to aid in movement through the water (Samuels and Van Valkenburgh, 2008). These characteristics hold true for *Castor canadensis* and *C. californicus* (Table 17, Appendix 3, Figures 12 and 13).

The femur anteroposterior diameter (FeAPD) in *Castor canadensis* is low, exhibiting an extreme flattening of the femur while *C. californicus* exhibits a more robust anteroposterior diameter than *C. canadensis*. The femoral epicondylar breadth (FeEB) is wider in *C. californicus* than in *C. canadensis*. A wider FeEB would allow for greater muscle attachments to help with swimming (Samuels and Van Valkenburgh, 2008) and would be expected in an animal of larger body mass. The anteroposterior and mediolateral diameters at the distal end of the tibia (TDEAPD and TDEMLD) are slightly wider in *C. californicus* than in *C. canadensis*, suggesting that *C. californicus* had more robust articular distal ends on the hindlimbs than *C. canadensis*. In the pes, the anteroposterior diameter of the third metatarsal (MT3APD) and mediolateral diameter of the fourth metatarsal (MT4MLD) are both more robust in *C. californicus* than *C. canadensis*. Increasing the size of the pes can aid in enlarging the surface area of the hindfoot for amplified propulsion through the water (Samuels and Van Valkenburgh, 2008), which would also be expected at larger body mass. The articular width

at the distal end of the humerus (HDAW) is wider in *C. californicus* than *C. canadensis*, suggesting that *C. californicus* had more robust articular distal ends on the forelimbs than *C. canadensis*, which would accommodate larger size and may have allowed a wider range of motions used in both swimming and digging.

Ecological Role and Taxonomic Validity of *Castor californicus*

Overall, analyses employed here have documented strong morphological similarity between the late Miocene to early Pleistocene-aged beaver *Castor californicus* and the extant North American beaver *C. canadensis*. Both taxa show high degrees of variability in size, and substantial overlap in both skull (cranium and dentary) and postcranial size and shape. Subtle, but notable morphological differences in the skull of *C. californicus* include a wider occiput and posteriorly positioned orbit (Figure 15). Dentary morphology in *C. californicus* displays distinctly wider separation between condylar and angular processes and anteroventrally depressed incisor alveolus (Figure 15). Postcranial morphology of *C. californicus* is distinguished from extant species of beaver by less dorsoventrally flattened the femur, greater robustness of hindlimb elements, and greater metatarsal widths. These differences may be attributable to body size and allometry, but do not likely represent substantial differences in function of either the cranial or postcranial skeleton.

Further comparisons between beaver species are necessary for a rigorous evaluation of the taxonomic validity of *Castor californicus*. Detailed examination of dental dimensions, occlusal patterns, and how teeth change ontogenetically would supplement the findings of this study. Additionally, including more *C. californicus*, modern *C. fiber*, and Pleistocene-aged *C. canadensis* and *C. fiber* specimens will help provide a better representative sample for future analyses. When combined, that would allow more confidence in assessing the validity of species. Our findings are consistent with *Castor californicus* and *C. canadensis* representing chronospecies, with subtle differences in morphology because of anagenetic changes in beavers over the last 7 million years. That time interval includes dramatic changes in climate, floras, and faunas in North America and the rest of the world (e.g., Webb, 1977; Graham, 1999; Jacobs et al., 1999; Janis et al., 2002; Retallack, 2007; Edwards et al., 2010; Stromberg, 2011; Samuels and Hopkins, 2017; Westerhold et al., 2020), and thus

some evolutionary changes within persisting lineages should not be surprising. Other well-studied rodents of North America have been interpreted similarly (anagenetic changes in a lineage, sometimes with recognizable chronospecies or subspecies). For example, muskrats (*Ondatra zibethicus*) are common in the fossil record and what were formerly considered distinct species are now treated as chrono-subspecies in a lineage that evolved greatly over the Pliocene and Pleistocene (Martin et al., 1996; Martin, 2019).

Regardless of taxonomic assignments of specimens, the strong morphological similarity of these two beaver species indicates they can be considered ecological analogs, having similar dietary and locomotor ecology. This is also what had been noted in prior ecomorphological studies of rodents, which inferred the ecology of *Castor californicus* to have been a semi-aquatic herbivore specialized for feeding on fibrous plant matter (Samuels and Van Valkenburgh, 2008; Samuels, 2009). Consequently, we can confidently infer the impacts of beavers on ecosystems in North America (i.e., tree-felling, dam building, watershed altering) to have been occurring since the late Miocene, at least 7 m.y.a. (Rybczynski, 2008; Samuels and Zancanella, 2011). Ongoing studies of beaver evolution and distribution will improve understanding of how both beavers and the ecosystems they inhabit have changed through time.

REFERENCES

Brazier, R.E., Puttock, A., Graham, H.A., Auster, R.E., Davies, K.H., and Brown, C.M.L. 2020. Beaver: Nature's ecosystem engineers. WIREs Water, 8:1.
https://doi.org/10.1002/wat2.1494

Calede, J.J. 2022. The oldest semi-aquatic beaver in the world and a new hypothesis for the evolution of locomotion in Castoridae. Royal Society Open Science, 9(8):220926.
https://doi.org/10.1098/rsos.220926

Cope, D.A. and Lacy, M.G. 1995. Comparative application of the coefficient of variation and range-based statistics for assessing the taxonomic composition of fossil samples. Journal of Human Evolution, 29:549-579.
https://doi.org/10.1006/jhev.1995.1075

Danilov, P.I., Kanshiev, V.Y., and Fedorov, F.V. 2011. Differences of the morphology of the North American and Eurasian beavers in Karelia, pp. 50-54. In Sjöberg, G. and Ball, J.P. (eds.), Restoring the Eurasian beaver: 50 years of experience. Pensoft Publishers, Sofia, Bulgaria.

Edwards, E.J., Osborne, C.P., Strömberg, C.A.E., Smith, S.A., and Consortium, C.G. 2010. The origins of C4 grasslands: integrating evolutionary and ecosystem science. Science, 328:587-591.
https://doi.org/10.1126/science.1177216

Emery-Wetherell, M.M. and Davis, E.B. 2018. Dental measurements do not diagnose modern artiodactyl species: Implications for the systematics of Merycoidodontoidea. Palaeontologia Electronica, 21.2.23A:1-28.
https://doi.org/10.26879/748

Flynn, L.J. and Jacobs, L.L. 2008. Castoroidea, pp. 391-405. In Janis, C.M., Gunnell, G.F., and Uhen, M.D. (eds.), Evolution of Tertiary Mammals of North America, Volume 2: Small Mammals, Xenarthrans, and Marine Mammals. Cambridge University Press, Cambridge, UK.

Gibbard, P.L. and Head, M.J. 2010. The newly-ratified definition of the Quaternary system/period and redefinition of the Pleistocene series/epoch, and comparison of proposals advanced prior to formal ratification. Episodes Journal of International Geosciences, 33(3):152-158.
https://doi.org/10.18814/epiiugs/2010/v33i3/002

Gingerich, P.D. 2003. Land-to-sea transition in early whales: evolution of Eocene Archaeoceti (Cetacea) in relation to skeletal proportions and locomotion of living semiaquatic mammals. Paleobiology, 29:429-454.
https://doi.org/10.1666/0094-8373(2003)029<0429:LTIEWE>2.0.CO;2

Graham, A. 1999. Late Cretaceous and Cenozoic History of North American Vegetation (North of Mexico). Oxford University Press, New York.
https://doi.org/10.1093/oso/9780195113426.001.0001

Halley, D.J., Saveljev, A.P., and Rosell, F. 2020. Population and distribution of beavers *Castor fiber* and *Castor canadensis* in Eurasia. Mammal Review, 51:1-24.
https://doi.org/10.1111/mam.12216

Hay, O.P. 1927. The Pleistocene mammals of the Western Region of North America and its Vertebrated Animals. Carnegie Institute of Washington, Washington D.C.

Hinze, G. 1950. Der Biber: Körperbau und Lebensweise. Verbreitung und Geschichte. Akademie Verlag, Berlin, Germany.

Horn, S., Durka, W., Wolf, R., Ermala, A., Stubbe, A., Stubbe, M., and Hofreiter, M. 2011. Mitochondrial genomes reveal slow rates of molecular evolution and the timing of speciation in beavers *(Castor),* one of the largest rodent species. PLoS ONE, 6(1):e14622.
https://doi.org/10.1371/journal.pone.0014622

Howell, A.B. 1930. Aquatic mammals; their adaptations to life in the water. Dover Publications, New York.
https://doi.org/10.5962/bhl.title.6582

Hugueney, M. 1999. Family Castoridae, pp. 1-516. In Rössner, G.E. and Heissig, K. (eds.). The Miocene land mammals of Europe. Verlag Friedrich Pfeil, München, Germany.

Jacobs, B.F., Kingston, J.D., and Jacobs, L.L. 1999. The origins of grass-dominated ecosystems. Annals of the Missouri Botanical Garden, 86(2):590-643.
https://doi.org/10.2307/2666186

Janis, C.M., Damuth, J., and Theodor, J.M. 2002. The origins and evolution of the North American grassland biome: The story from the hoofed mammals. Palaeogeography, Palaeoclimatology, Palaeoecology, 177:183-198.
https://doi.org/10.1016/S0031-0182(01)00359-5

Jenkins, S.H. and Busher, P.E. 1979. *Castor canadensis*. Mammalian Species, 120:1-8.
https://doi.org/10.2307/3503787

Kauhala, K. and Timonen, P. 2016. Mitä majavien kallot kertovat? Suomen Riista, 62:7-18. (In Finnish, with English summary)

Kellogg, L. 1911. A fossil beaver from the Kettleman Hills, California. University of California Press, 6:401-402.

Koch, P.L. 1986. Clinal geographic variation in mammals: implications for the study of chronoclines. Paleobiology, 12(3):269-281.
https://doi.org/10.1017/S0094837300013774

Korth, W.W. 1994. The Tertiary record of rodents in North America. Springer, New York.
https://doi.org/10.1007/978-1-4899-1444-6

Korth, W.W. and Samuels, J.X. 2015. New rodent material from the John Day Formation (Arikareean, middle Oligocene to early Miocene) of Oregon. Annals of Carnegie Museum, 83(1):19-84.
https://doi.org/10.2992/007.083.0102

Kurtén, B. and Anderson, E. 1980. Pleistocene mammals of North America. Columbia University Press, New York.

Long, K. 2000. Beaver: a wildlife handbook. Johnson Books, Boulder, Colorado.

Martin, J.M., Mead, J.I., and Barboza, P.S. 2018. Bison body size and climate change. Ecology and Evolution, 8:4564-4574.
https://doi.org/10.1002/ece3.4019

Martin, L.D. 1989. Plio-Pleistocene rodents in North America. In series: Black, C.C. and Dawson, M.R. (eds.), Papers on fossil rodents in honor of Albert Elmer Wood, Science Series 33. Natural History Museum of Los Angeles County, Los Angeles, California.

Martin, L.D. and Bennett, D. 1977. The burrows of the Miocene beaver *Palaeocastor*, Western Nebraska, U.S.A. Palaeogeography, Palaeoclimatology, Palaeoecology, 22:173-193.
https://doi.org/10.1016/0031-0182(77)90027-X

Martin, R.A. 2019. Body mass and correlated ecological variables in the North American muskrat lineage: evolutionary rates and the tradeoff of large size and speciation potential. Historical Biology, 31(5):631-643.
https://doi.org/10.1080/08912963.2017.1384474

Martin, R.A., Stewart, K., and Seymour, K. 1996. Dental evolution and size change in the North American muskrat: classification and tempo of a presumed phyletic sequence, pp. 431-457. Palaeoecology and Palaeoenvironments of Late Cenozoic Mammals: Tributes to the Career of CS (Rufus) Churcher. University of Toronto Press, Toronto, Ontario.

Monteiro, L.R., Bonato, V., and dos Reis, S.F. 2005. Evolutionary integration and morphological diversification in complex morphological structures: mandible shape divergence in spiny rats (Rodentia, Echimyidae). Evolution Development, 7:429-439.
https://doi.org/10.1111/j.1525-142X.2005.05047.x

Retallack, G.J. 2007. Cenozoic paleoclimate on land in North America. The Journal of Geology, 115:271-294. https://doi.org/10.1086/512753

Rhoads, S.N. 1898. Contributions to a revision of the North American beavers, otters and fishers. Transactions of the American Philosophical Society, 19:417-439.
https://doi.org/10.2307/1005498

Robertson, R.A. and Shadle, A.R. 1954. Osteologic criteria of age in beavers. Journal of Mammalogy, 35:197-203.
https://doi.org/10.2307/1376033

Rosell, F., Bozer, O., Collen, P., and Parker, H. 2005. Ecological impact of beavers *Castor fiber* and *Castor canadensis* and their ability to modify ecosystems. Mammal Review, 35:248-276.
https://doi.org/10.1111/j.1365-2907.2005.00067.x

Rohlf, F.J. 2011. tpsRegr, shape regression, version 1.40. State University of New York at Stony Brook, Department of Ecology and Evolution.

Rohlf, F.J. 2015a. The tps series of software. Hystrix, the Italian Journal of Mammalogy, 26:1-4.
https://doi.org/10.4404/hystrix-26.1-11264

Rohlf, F.J. 2015b. tpsRelw: relative warps analysis. State University of New York at Stony Brook, Department of Ecology and Evolution.

Rohlf, F.J. 2021. tpsDig2, version 2.31. State University of New York at Stony Brook, Department of Ecology and Evolution.

Rybczynski, N. 2007. Castorid phylogenetics: Implications for the evolution of swimming and tree-exploitation in beavers. Journal of Mammalian Evolution, 14:1-35.
https://doi.org/10.1007/s10914-006-9017-3

Rybczynski, N. 2008. Woodcutting behavior in beavers (Castoridae, Rodentia): estimating ecological performance in modern and fossil taxon. Paleobiology, 34:389-402.
https://doi.org/10.1666/06085.1

Rybczynski, N., Ross, E.M., Samuels, J.X., and Korth, W.W. 2010. Re-evaluation of *Sinocastor* (Rodentia: Castoridae) with implications on the origin of modern beavers. PLoS ONE, 5:e13990.
https://doi.org/10.1371/journal.pone.0013990

Samuels, J.X. 2009. Cranial morphology and dietary habits of rodents. Zoological Journal of the Linnaean Society, 156: 864-888.
https://doi.org/10.1111/j.1096-3642.2009.00502.x

Samuels, J.X. and Hopkins, S.S.B. 2017. The impacts of Cenozoic climate and habitat changes on small mammal diversity of North America. Global and Planetary Change, 149:36-52.
https://doi.org/10.1016/j.gloplacha.2016.12.014

Samuels, J.X. and Van Valkenburgh, B. 2008. Skeletal indicators of locomotor adaptations in living and extinct rodents. Journal of Morphology, 269:1387-1411.
https://doi.org/10.1002/jmor.10662

Samuels, J.X. and Van Valkenburgh, B. 2009. Craniodental adaptations for digging in extinct burrowing beavers. Journal of Vertebrate Paleontology, 29:254-268.
https://doi.org/10.1080/02724634.2009.10010376

Samuels, J.X. and Zancanella, J. 2011. An early Hemphillian occurrence of *Castor* (Castoridae) from the Rattlesnake Formation of Oregon. Journal of Paleontology, 85:930-935.
https://doi.org/10.1666/11-016.1

Segura, V., Flores, D., and Deferrari, G. 2023. Comparison of skull growth in two ecosystem modifiers: beavers *Castor canadensis* (Rodentia: Castoridae) and muskrats *Ondatra zibethicus* (Rodentia: Cricetidae). Zoologischer Anzeiger, 304:61-72. https://doi.org/10.1016/j.jcz.2023.03.004

Shotwell, J.A. 1970. Pliocene mammals of Southeast Oregon and adjacent Idaho. Bulletin of the Museum of Natural History, University of Oregon, Eugene, Oregon, 17:1-103.

Sokal, R.R. and Braumann, C.A. 1980. Significance tests for coefficients of variation and variability profiles. Systematic Zoology, 29:50-66. https://doi.org/10.1093/sysbio/29.1.50

Stefen, C. 2009. Intraspecific variability of beaver teeth (Castoridae: Rodentia). Zoological Journal of the Linnean Society, 155(4):926-936. https://doi.org/10.1111/j.1096-3642.2008.00467.x

Stefen, C. 2010. Morphometric considerations of the teeth of the palaeocastorine beavers *Capacikala, Palaeocastor* and *"Capatanka".* Palaeontologia Electronica, 13(1):1-34. https://palaeo-electronica.org/2010_1/191/index.html

Stirton, R.A. 1935. A review of the Tertiary beavers. University of California Press, Berkeley, California.

Strömberg, C.A.E. 2011. Evolution of grasses and grassland ecosystems. Annual Review of Earth and Planetary Sciences, 39:517-544. https://doi.org/10.1146/annurev-earth-040809-152402

The NOW Community 2023. New and old worlds database of fossil mammals (NOW). Licensed under CC BY 4.0. Retrieved 05 July 2023 from https://nowdatabase.org/now/database/ http://doi.org/10.5281/zenodo.4268068

Troszyński, W. 1975. The main differences in the structure of the skull of both the Canadian beaver (*Castor canadensis* Kuhl) and the European beaver (*Castor fiber* Linnaeus). Przegląd Zoologiczny, 19:481-486.

Webb, S.D. 1977. A history of savanna vertebrates in the New World. Part I. North America. Annual Review of Ecology and Systematics, 8:355-380. https://doi.org/10.1146/annurev.es.08.110177.002035

Westerhold, T., Marwan, N., Drury, A.J., Liebrand, D., Agnini, C., Anagnostou, E., Barnet, J.S.K., Bohaty, S.M., De Vleeschouwer, D., Florindo, F., Frederichs, T., Hodell, D.A., Holbourn, A.F., Kroon, D., Lauretano, V., Littler, K., Lourens, L.J., Lyle, M., Pälike, H., Röhl, U., Tian, J., Wilkens, R.H., Wilson, P.A., and Zachos, J.C. 2020. An astronomically dated record of Earth's climate and its predictability over the last 66 million years. Science, 369(6509):1383-1387. http://doi.org/10.1126/science.aba6853

Zakrzewski, R.J. 1969. The rodents from the Hagerman local fauna, Upper Pliocene of Idaho. Museum of Paleontology, University of Michigan, Ann Arbor, Michigan.

APPENDIX 1.

Cranial specimens used in geometric morphometric analysis. Available for download at https://palaeo-electronica.org/content/2023/3943-fossil-beaver-morphology.

APPENDIX 2.

Dentary specimens used in geometric morphometric analysis. Available for download at https://palaeo-electronica.org/content/2023/3943-fossil-beaver-morphology.

APPENDIX 3.

Postcranial specimens and measurements. Available for download at https://palaeo-electronica.org/content/2023/3943-fossil-beaver-morphology.